

الجمهورية الجزائرية الديمقراطية الشعبية

**REPUBLIQUE ALGERIENNE DEMOCRATIQUE ET POPULAIRE**

وزارة التعليم العالي والبحث العلمي

**Ministère de l'Enseignement Supérieur et de la Recherche Scientifique**

جامعة أبي بكر بلقايد - تلمسان

Université Aboubakr Belkaïd – Tlemcen –

Faculté de TECHNOLOGIE



**THESE**

Présentée pour l'obtention du **grade** de **DOCTORAT 3ème Cycle**

**En** : Hydraulique

**Spécialité** : Science et technologie hydraulique

**Par** : Mr Afra Abdallah

**Sujet**

**Modeling for Flood Risk Management : Cartographic Approach/  
Modélisation pour la gestion du risque inondation : Approche  
Cartographique**

Soutenue publiquement, le / / , devant le jury composé de :

Mr GHENIM Abderrahmane Nekkache	Professeur	Univ. Tlemcen	Président
Mr MEGNOUNIF Abdesselam	Professeur	Univ. Tlemcen	Directeur de thèse
Mme Abdelbaki Chérifa	Professeur	Univ. Tlemcen	Co- Directeur de thèse
Mr Baahmed Djelloul	Professeur	Univ. Sidi Bel Abbès	Examineur 1
Mme Gherissi Radia	MCA	C.Univ. Maghnia	Examineur 2
Mr Saber Mohamed	Dr	Univ. Kyoto, Japon	Invité

# **Dedication**

With utmost dedication, I dedicate this humble work to my dear father and caring mother. Their unwavering support has always been the foundation of my efforts, and this achievement stands as a testimony to their unwavering faith in me. I also dedicate it to my brothers who have helped me at every stage of my life. As for my dear wife, no dedication can fully express the profound respect, undying love and profound gratitude I have for you. It remains my ambition to never waver in living up to your expectations and those of all my friends and colleagues.

## **ACKNOWLEDGEMENT**

Primarily, I express my profound gratitude to Allah Almighty for bestowing upon me the fortitude and wisdom necessary to accomplish this endeavor. I wish to convey my profound gratitude to my supervisor and co-supervisor, Professor MEGNOUNIF Abdesselam and Professor ABDELBAKI Chérifa, for their steadfast support, encouragement, invaluable guidance, patience, insightful suggestions, and professional counsel throughout the completion of this PhD thesis. Their profound expertise across multiple disciplines has significantly enhanced this endeavor, and I am privileged to have had them as my supervisors.

I wish to convey my heartfelt appreciation to Dr. Mohammed Abdel-Fattah from Kyoto University for his invaluable professional guidance, technical support, assistance, and encouragement.

I extend my profound gratitude to my esteemed colleagues, Dr. Berezzel Yacine and Dr. Benabdelkrim Amine, for their steadfast support, encouragement, and invaluable guidance throughout the completion of my thesis.

I am profoundly appreciative of my family, particularly my father, who was the inaugural individual to confer upon me the title of "Doctor." I would like to extend my sincere gratitude to my siblings for their unwavering support and invaluable encouragement throughout the process of completing my thesis. I express my profound gratitude to my esteemed wife, my foremost supporter, and I thank her for her unwavering fortitude and invaluable assistance.

**Abstract :**

This PhD dissertation examines flood risk assessment in Algeria's Mekerra Basin utilising an advanced Rainfall-Runoff-Inundation (RRI) modelling methodology to overcome significant deficiencies in flood prediction and management for semi-arid locations. The research establishes an extensive hydrological modelling framework that incorporates high-resolution topography data, land use patterns, and historical climate records to simulate and forecast flood dynamics under present climatic scenarios. The RRI model exhibits robust predictive performance ( $NSE > 0.86$ ,  $R^2 > 0.89$ ) in accurately representing the basin's distinctive flash flood behaviour, as evidenced by thorough calibration and validation against recorded flood events. This research not only advances the field of semi-arid hydrology but also offers policy recommendations that bolster Algeria's national flood risk reduction strategies, while creating a transferable methodology applicable to other data-scarce regions susceptible to heightened flood risks due to climate change. The results underscore the pressing necessity for adaptive water management strategies that integrate sophisticated modelling methods with community-driven mitigation efforts to improve resilience in the Mekerra Basin and similar semi-arid watersheds globally.

**Keywords:** flood modeling; Rainfall–Runoff–Inundation (RRI) model; Mekerra Basin; flood risk assessment; semi-arid

## **Résumé :**

Cette thèse de doctorat examine l'évaluation des risques d'inondation dans le bassin de la Mekerra en Algérie. Elle utilise une méthodologie avancée de modélisation pluie-débit-inondation (RRI) pour pallier les importantes lacunes en matière de prévision et de gestion des inondations dans les zones semi-arides. La recherche établit un cadre de modélisation hydrologique complet qui intègre des données topographiques haute résolution, des schémas d'occupation du sol et des relevés climatiques historiques pour simuler et prévoir la dynamique des inondations selon les scénarios climatiques actuels et futurs. Le modèle RRI présente de solides performances prédictives ( $NSE > 0,86$ ,  $R^2 > 0,89$ ) en représentant avec précision le comportement particulier des crues éclair du bassin, comme en témoignent un étalonnage et une validation approfondis par rapport aux inondations enregistrées. Cette recherche fait non seulement progresser le domaine de l'hydrologie semi-aride, mais propose également des recommandations politiques qui renforcent les stratégies nationales algériennes de réduction des risques d'inondation, tout en créant une méthodologie transférable applicable à d'autres régions pauvres en données et exposées à des risques accrus d'inondation en raison du changement climatique. Les résultats soulignent la nécessité urgente de stratégies de gestion adaptative de l'eau qui intègrent des méthodes de modélisation sophistiquées avec des efforts d'atténuation menés par la communauté pour améliorer la résilience dans le bassin de Mekerra et dans les bassins versants semi-arides similaires à l'échelle mondiale.

**Mots-clés :** modélisation des inondations ; modèle pluie-ruissellement-inondation (RRI) ; bassin de Mekerra ; évaluation des risques d'inondation ; semi-aride.

## ملخص:

تتناول هذه الأطروحة للدكتوراه تقييم مخاطر الفيضانات في حوض نهر ميكيرا بالجزائر. وتستخدم منهجية متقدمة لنمذجة هطول الأمطار والجريان السطحي والفيضانات (RRI) لمعالجة الثغرات الكبيرة في التنبؤ بالفيضانات وإدارتها في المناطق شبه القاحلة. يُؤسس البحث إطارًا شاملاً للنمذجة الهيدرولوجية يدمج بيانات طبوغرافية عالية الدقة، ومخططات الغطاء الأرضي، وسجلات المناخ التاريخية لمحاكاة ديناميكيات الفيضانات والتنبؤ بها في ظل سيناريوهات المناخ الحالية والمستقبلية. يُظهر نموذج RRI أداءً تنبؤيًا قويًا ( $R^2 > 0.89$ ,  $NSE > 0.86$ ) من خلال تمثيل دقيق للسلوك المحدد للفيضانات المفاجئة في الحوض، كما يتضح من خلال معايرة شاملة وتحقق من صحة النتائج باستخدام الفيضانات المسجلة. لا يُسهم هذا البحث في تطوير مجال الهيدرولوجيا شبه القاحلة فحسب، بل يُقدم أيضًا توصيات سياساتية تُعزز استراتيجيات الجزائر الوطنية للحد من مخاطر الفيضانات، مع إنشاء منهجية قابلة للتطبيق في مناطق أخرى تقتقر إلى البيانات وتتعرض لمخاطر فيضانات متزايدة نتيجة لتغير المناخ. تؤكد النتائج على الحاجة الملحة إلى استراتيجيات مُتكيفة لإدارة المياه، تُدمج أساليب النمذجة المُتطورة مع جهود التخفيف التي تقودها المجتمعات المحلية، لتعزيز القدرة على الصمود في حوض ميكيرا وأحواض الأنهار شبه القاحلة المُماثلة على مستوى العالم.

الكلمات المفتاحية: نمذجة الفيضانات؛ نموذج هطول الأمطار والجريان السطحي والفيضانات؛ حوض ميكيرا؛ تقييم مخاطر الفيضانات؛ شبه قاحله

## **LIST OF TABLES**

Table 2.1: Inventory of tragic floods in Algeria.

Table 2.2: Human casualties associated with flood episodes in the Wadi Mekerra basin (1986–2007).

Table 3.1: Morphometric parameters.

Table 4.1: RRI cases and limits of operation of these parameters.

Table 5.1 :RRI parameter value of calibration.

Table 5.2: RRI model performance metrics for calibration and validation.

## LIST OF FIGURES

Figure 1.1: flood sidi bel abbas.

Figure 2.1: Coastal flooding in Scilla.

Figure 2.2: River floods (fluvial floods).

Figure 2.3: The scene of an urban flood in Taiwan.

Figure 2.4: Damage caused by flash floods in Wenchuan, china.

Figure 2.5: The affected areas by flash floods in MENA region.

Figure 2.6: Flood of Ain Sefra southwest of Algeria on September 7, 2024.

Figure 2.7: flood damage in In Guezzam city in August 2018.

Figure 2.8: Schematic diagram of the Tank model

Figure 2.9: Schematic diagram of Physical model

Figure 3.1: Location of Mekerra watershed.

Figure 3.2: Sub-bassins of mekerra.

Figure 3.3: Stream order of mekerra.

Figure 3.4: mekerra land cover.

Figure 3.5: soil types map of the Mekerra watershed.

Figure 4.1: diagram of Rainfall Runoff Inundation (RRI) Model.

Figure 4.2: Flowchart illustrating the configuration procedure of the RRI model. Figure 4.3: Methods for preparing rainfall data for entry into the RRI model.

Figure 4.4: DEM mekerra.

Figure 4.5: Flow direction Mekerra.

Figure 4.6: Flow accumulation mekerra.

Figure 4.7: Example of land use in ascii format.

Figure 4.8: Flow diagram illustrating the methodology for applying the Rainfall–Runoff–

Inundation (RRI) model in the Mekerra Basin study.

Figure 4.9: The program interface and where values are changed during the calibration and validation process

Figure 4.10: RRI cases.

Figure 5.1: Simulated hydrograph variations of vertical saturated hydraulic conductivity (Ksv).

Figure 5.2: Simulated hydrograph variations of suction at the vertical wetting front (Sf).

Figure 5.3: Simulated hydrograph variations channel roughness coefficient (ns\_river)

Figure 5.4: Simulation of Mekerra flash flood event RRI model calibration results for 1986 event.

Figure 5.5: Simulation of Mekerra flash flood event RRI model validation results for 1994 event.

Figure 5.6 : Simulation of September 1994 flood event : (a) Runge–Kutta model simulation results; (b) RRI model simulation results Runge–Kutta model simulation results.

## **APPENDIX**

Table 2.3: Detailed description of conceptual, physical and empirical models

Appendix A1: simulation of runoff (Mekerra watershed) using RRI model.

Appendix A2: water depth and river discharge using RRI model.

## LIST OF ABBREVIATIONS

**(A)** watershed area

**(AI)** artificial intelligence

**(ANRH)** The National Agency of Hydraulic Resources

**(CUI)** Command User Interface

**(Dd)** Drainage density

**(DEMs)** Digital Elevation Models

**(FAO)** Food and Agriculture Organization

**(Gamma)** Soil porosity

**(Gammam)** Unsaturation effective porosity

**(GIS)** Geographic Information Systems

**(GLUE)** Generalized Likelihood Uncertainty Estimation method

**(GUI)** Graphical User Interface

**(Ish)** Inverse shape form

**(Ka)** Lateral saturated hydraulic conductivity

**(Kg)** Compactness index

**(Kv)** Vertical saturated hydraulic conductivity

**(LULC)** land use and land covers

**(MENA)** Middle East and North Africa region

**(ML)** machine learning

**(ns\_river)** Channel roughness coefficient

**(ns\_slope)** Hillslope roughness coefficient

**(NSE)** The Nash–Sutcliffe Efficiency

**(Pr)** Perimeter of the basin

**(QdF)** Flow–Duration–Frequency model

**(RKDG)** Runge-Kutta Discontinuous Galerkin model

**(Rn)** Ruggedness number

**(Rr)** Relief ratio

**(RRI)** Rainfall Runoff Inundation

**(RS)** remote sensing

**(Sfr)** Stream frequency

**(Sf)** Suction at the vertical wetting front

**(Soilepth)** Soil depth

**(SRTM)** Shuttle Radar Topography Mission

**(TM)** Thematic Mapper

**(Tr)** Texture ratio

**(UNDRR)** The United Nations Office for Disaster Risk Reduction

**(WMO)** World Meteorological Organization

# TABLE OF CONTENTS

## CHAPTER 1 INTRODUCTION

1.1 Background and context of the study.....	06
1.2 Problem statement.....	08
1.3 Objectives of the research.....	09
1.4 Significance of the study.....	10
1.5 Overview of the dissertation structure.....	11

## CHAPTER 2 LITERATURE REVIEW

2.1 Introduction.....	13
2.2 Flood definition.....	13
2.3 Different types of flood.....	13
2.3.1 Coastal flood.....	13
2.3.2 Fluvial floods.....	14
2.3.3 Urban flood.....	15
2.3.4 Flash flood.....	16
2.4 Flood risk in MENA region.....	17
2.5 Floods risk in Algeria.....	19
2.6 Flash floods risk in Algeria.....	19
2.7 Flood risk in mekerra.....	22
2.8 Rainfall-Runoff Models.....	23
2.9 Rationale for selecting physical models.....	27

2.10 Reasons the RRI Model is the optimal selection.....	28
2.11 Demonstrated Efficacy in Comparable Situations.....	29
2.12 Previous studies.....	29
2.13 Constraints of Alternative Physical Models.....	31

## **CHAPTER 3            STUDY AREA**

3.1 Introduction.....	33
3.2 Geographical Location and Boundaries.....	33
3.3 Geomorphological Characteristics.....	34
3.3.1 Watershed area.....	36
3.3.2 Perimeter of the basin.....	37
3.3.3 Stream frequency.....	37
3.3.4 Drainage density (Dd).....	39
3.3.5 Inverse shape form (Ish).....	40
3.3.6 Relief ratio (Rr).....	41
3.3.7 Ruggedness number (Rn).....	41
3.3.8 Texture ratio (Tr).....	42
3.3.9 Compactness index (Kg).....	43
3.4 Climate and Meteorological Conditions.....	44
3.5 Hydrological Characteristics.....	45
3.5.1 Hydrographic network.....	45
3.6 Land Use and Land Cover.....	45

3.7 Soil Types and Characteristics.....	46
3.8 CONCLUSION.....	48

## **CHAPTER 4      METHODOLOGY**

4.1 Introduction.....	50
4.2 Data collection.....	50
4.2.1 Rainfall and Runoff Data.....	50
4.2.2 Topographic and Watershed Data.....	51
4.2.3 Land use.....	52
4.3 Modeling.....	52
4.3.1 ArcGIS.....	52
4.3.2 Rainfall-Runoff Inundation Model.....	53
4.3.2.1 RRI Model Description.....	53
4.3.2.2 RRI Model Input and Set-Up.....	55
4.3.2.3 RRI Model Application.....	59
4.3.2.4 calibration and validation.....	61
4.4 Limitations of the methodology.....	65
4.5 Conclusion.....	65

## **CHAPTER 5:      RESULTS AND DISCUSSION**

5.1 Introduction.....	67
5.2 Sensitivity Analysis.....	67
5.3 Calibration and Validation Results.....	71

5.4 Simulation of Mekerra Flash Flood Event.....73

5.5 Comparison with other models used Mekerra basin.....76

5.6 Conclusion.....78

**CHAPTER 6: CONCLUSIONS**

6.1 CONCLUSION.....81

6.2 Recommendations.....82

REFERENCES..... 83

APPENDIX.....99

# *Chapter 1:*

# Introduction

## **1.1 Background and context of the study**

Floods rank among the most catastrophic natural disasters worldwide, resulting in considerable fatalities, infrastructure destruction, and economic turmoil (Lee et al., 2020). The United Nations Office for Disaster Risk Reduction (UNDRR) reports that floods constitute almost 40% of all global natural catastrophes, impacting more than 2 billion individuals from 1998 to 2017 (UNDRR, 2020). The necessity of combating floods is becoming increasingly urgent due to their catastrophic effects on human lives, infrastructure, and ecosystems (Petrochenko, 2023). The rising frequency and severity of flood events, influenced by climate change, urbanization, and alterations in land use, have intensified the necessity for precise flood risk evaluation and management measures. Flood risk assessment is analyzing the probability and possible consequences of flooding, which is crucial for formulating effective mitigation strategies and bolstering community resilience (Han et al., 2024; Liu et al., 2023).

Flood is a multifaceted phenomenon affected by numerous interconnected elements, such as hydrodynamic processes. Comprehending these intricacies is essential for proficient flood management (S. Lee et al., 2023).

Recent years have seen a significant transformation in flood control studies, encompassing flood hazard mapping, remote sensing (RS), machine learning (ML), artificial intelligence (AI), and hydrological modeling. These strategies vary on the input data required and the outcomes produced (Brunner et al., 2021; Karim et al., 2023; Kumar et al., 2023 ; Mudashiru et al., 2021; Munawar et al., 2022).

Algeria, situated in North Africa, is particularly susceptible to flooding owing to its semi-arid environment, marked by erratic and heavy precipitation occurrences (Boutaghane et al., 2021; Hafnaoui et al., 2023). The nation has endured multiple devastating floods in recent decades, notably the 2001 Bab El Oued flood in Algiers, which caused more than 700 deaths and significant destruction to property and infrastructure (Sardou & Petrucci, 2023).

The Mekerra Basin, situated in northwestern Algeria, is especially susceptible to flooding owing to its steep topography, heavy seasonal precipitation, and swift urban development. Floods in the Mekerra Basin have resulted in considerable socio-economic repercussions, including fatalities,

devastation of agricultural land, and disruption of local populations (fig 1.1) (Korichi et al., 2016).

The Mekerra Basin encompasses over 3000 km<sup>2</sup> and is distinguished by a Mediterranean climate featuring wet winters and arid summers. The basin serves as a crucial agricultural and economic center, sustaining local populations through agriculture and livestock (Atallah et al., 2024). Precise flood risk evaluation in the Mekerra Basin is essential for guiding land-use planning, emergency readiness, and climate adaption initiatives.

Rainfall-Runoff-Inundation (RRI) models have become effective instruments for simulating flood dynamics and evaluating flood risk. These models incorporate precipitation, runoff, and flooding dynamics, delivering comprehensive spatial and temporal data on flood extent, depth, and duration (Jehanzaib et al., 2022). The RRI model, created by Sayama et al. (2012), is especially appropriate for areas with intricate topography and fluctuating rainfall patterns, rendering it an optimal selection for the Mekerra Basin. In contrast to conventional hydrological models, the RRI model is capable of simulating both surface runoff and subsurface flow, providing a more thorough comprehension of flood dynamics.

Notwithstanding the increasing utilization of hydrological models in flood risk evaluation, substantial deficiencies persist in the current research, especially in semi-arid areas such as Mekerra.

This study intends to employ the Rainfall Runoff Inundation (RRI) model to deliver a thorough evaluation of flood risk in the Mekerra Basin. This research will improve flood risk predictions by including rainfall data, runoff dynamics, and inundation processes, resulting in a more comprehensive understanding of flood stages and precise information throughout the basin to guide regional flood control plans.



Fig1.1: flood sidi bel abbas September 14, 2018 (source <https://bel-abbes.info/sidi-bel-abbes-des-inondations-encore-des-inondations/>)

## 1.2 Problem statement

Flash floods are disasters with a rising trend in both severity and frequency (Wang et al., 2023). Nonetheless, detailed studies on this phenomenon in Algeria are limited. The optimal timeframe for these floods was September, October, and November (Remini, 2023). Precise flood risk evaluation is essential for efficient flood management and catastrophe readiness. Nevertheless, numerous places encounter difficulties in evaluating flood risk owing to the constraints of existing methodologies and models. Conventional flood risk assessment methods frequently depend on historical flood data or rudimentary flood mapping techniques, which inadequately reflect the dynamic characteristics of flood episodes, especially in regions undergoing rapid urbanisation or facing heightened climate change effects.

The Mekerra Basin is especially susceptible to flooding owing to its intricate hydrological conditions, and insufficient drainage infrastructure. Notwithstanding prior attempts to evaluate flood risk in the area, current flood models frequently fail to accurately forecast flood dynamics due to data deficiencies, insufficient integration of rainfall, runoff, and inundation processes.. Moreover, these models lack the requisite detail for effective local flood risk management and decision-making.

The Rainfall-Runoff-Inundation (RRI) model, which synthesises rainfall, surface runoff, and flood inundation processes, presents a viable solution to these difficulties. This model facilitates a

more thorough comprehension of flood dynamics by incorporating local topography, land use, Nonetheless, there is an absence of region-specific RRI models in the Mekerra Basin, and the current models do not adequately address the intricate relationships between urban and rural flooding.

This study aims to formulate and implement an RRI model for an extensive flood risk evaluation in the Mekerra Wadi. The main aim of this work is to enhance flood hazard prediction, address deficiencies in existing flood risk assessment, and offer practical recommendations for flood risk management and policy formulation. This work use the RRI model to produce precise flood risk maps and decision-support tools for local authorities and stakeholders, thereby aiding in the mitigation of future flooding impacts.

### **1.3 Objectives of the research**

The primary aim of this research is to create and implement a Rainfall-Runoff-Inundation (RRI) model to evaluate flood risk in the Mekerra basin, offering a precise and comprehensive instrument for flood hazard forecasting and risk management. The explicit aims are as follows:

- 1- To formulate an RRI model that integrates the distinctive hydrological, topographical, and socio-economic attributes of Wadi Mekerra, encompassing local precipitation patterns, land use, and floodplain features.
- 2- To calibrate and validate the RRI model by juxtaposing its outputs with historical flood data, encompassing recorded rainfall, runoff, and inundation depths from previous flood occurrences.
- 3- To furnish pragmatic recommendations for municipal authorities, urban planners, and other stakeholders for flood risk management measures, derived from the outcomes of the flood risk assessment and model simulations.

#### **1.4 Significance of the study:**

This research on flood risk assessment employing the Rainfall-Runoff-Inundation (RRI) model in Wadi Mekerra offers substantial contributions to both scientific inquiry and practical flood risk management. The creation and implementation of a tailored RRI model will enhance the existing comprehension of flood dynamics in the region by providing a more cohesive and precise method for flood prediction. This is especially pertinent in quickly urbanising regions and in the face of escalating climate variability, when traditional flood models frequently prove inadequate.

This work will increase hydrological modelling by improving the integration of rainfall, runoff, and inundation processes. This innovative method will address a deficiency in the current literature, particularly on the application of inundation models to areas with intricate hydrological systems, notably in semi-arid regions. The results will possess interdisciplinary significance, influencing domains such as climate change research, environmental science, and urban planning.

The project will furnish essential data for local authorities, urban planners, and disaster management organisations to improve flood risk forecasting and decision-making. The flood hazard maps produced by the RRI model will facilitate the identification of flood-prone regions and the prioritisation of flood mitigation measures. These maps will aid in formulating climate adaption strategies, mitigating future flood hazards due to evolving climatic circumstances.

This research could substantially enhance flood resilience in the Mekerra Basin. The project will enhance local resilience, mitigate flood damage, and preserve lives and property by identifying at-risk communities and infrastructure. Furthermore, the advice generated from the model simulations may guide economical flood mitigation strategies, promoting sustainable development and minimising long-term economic losses.

This study's conclusions are pertinent to other flood-prone locations worldwide encountering analogous issues of urbanisation and climate change. The approaches and insights established herein may be applied to other regions, enhancing flood risk management practices globally. This project will enhance scientific knowledge and offer practical insights to better flood risk management and policy development in the Mekerra Basin and beyond.

## **1.5 Overview of the dissertation structure**

This dissertation is structured into the subsequent chapters:

**Chapter 1:** Introduction presents an overview of the study, encompassing the background, issue statement, aims, significance of the research, and a summary of the dissertation structure.

**Chapter 2:** Literature Review provides an examination of the current literature about flood classifications, floods within the study area, emphasising the models employed in this context. This research emphasises significant findings from other studies and delineates the gaps it aims to fill.

**Chapter 3:** Study Area delineates the case study region, encompassing its topographical, hydrological, and socio-economic attributes.

**Chapter 4:** Methodology Describes the technique employed in the study, encompassing the data utilised, such as rainfall, runoff, and topographic information, along with the problems faced during data gathering. The text elucidates the construction and calibration of the RRI model. This chapter delineates the model configuration, data processing procedures, and the simulations conducted to evaluate flood risk.

**Chapter 5:** Results and Discussion delineates the outcomes of the flood risk simulations, encompassing flood hazard maps and the demarcation of risk zones, and Analyses the findings within the framework of the research domain and the extensive literature. It examines the ramifications for flood risk management and assesses the applicability of the RRI model.

**Chapter 6:** Conclusions and Recommendations Summarises the principal findings of the study and provides recommendations for enhancing flood risk management in the case study region. It also examines the overarching significance of the research and proposes avenues for subsequent inquiry.

**The references** enumerate all sources cited in the dissertation.

*Chapter 2:*  
Literature Review

## **2.1 Introduction**

Floods pose a substantial hazard to populations and ecosystems globally, inflicting considerable damage to infrastructure, property, and resulting in loss of life. In flood-prone regions, it is essential to establish effective flood risk assessment methodologies to comprehend possible hazards and alleviate their effects. This research study utilises the Rainwater Inundation (RRI) model for flood risk evaluation. Furthermore, it offers a comprehensive overview of floods, encompassing their classifications, causative factors, and consequences. The text delineates flood threats in the MENA region, Algeria, and ultimately the research area.

The literature review elucidates prior research undertaken in Wadi Mekerra by detailing the methodologies employed, hence enhancing comprehension of the occurrence in the study area.

It also underscores prior studies on flood risk estimates that employed a comparable methodology from areas with varying climates.

## **2.2 Flood definition**

Floods, as defined by the World Health Organization, represent the most prevalent category of natural disaster, occurring when floodwaters inundate typically arid terrain. Floods are frequently precipitated by intense precipitation, swift snowmelt, or significant storm surges resulting from a tropical cyclone or tsunami in coastal regions.

## **2.3 Different type of flood**

Various varieties of floods exist, each possessing distinct characteristics and causes.

### **2.3.1 Coastal flood**

Coastal flooding predominantly occurs due to the convergence of storm surges and severe winds with elevated tides. The surge is attributable to elevated sea levels caused by low air pressure. In specific configurations, such as significant estuaries or enclosed marine regions, the accumulation of water is intensified by the combination of seabed shallowing and the impediment of return flow (WMO, 2011).

The possibility of coastal flooding is anticipated to increase in the future due to two primary factors. Firstly, global climate change and rising sea levels are anticipated to increase the frequency and intensity of flood occurrences; secondly, the number of potential receptors, including as infrastructure, socio-economic assets, and people, is growing in coastal regions (Ballesteros et al., 2017).



Fig 2.1 : Coastal flooding in Scilla. (Nucera et al. 2018)

### 2.3.2 Fluvial floods

Fluvial floods arise when a river exceeds its banks, resulting in the flooding of surrounding regions. Fluvial floods can result from various atmospheric processes, including monsoonal rainfall, landfalling hurricanes, and significant temperature increases that lead to snowmelt. (Merz et al. 2021)

Fluvial floods are notable among natural disasters due to their extensive prevalence, considerable damage, and regular occurrence. They pose a significant challenge in tackling climate change and

act as a considerable barrier to sustainable development, both directly and indirectly. The instability of climate complicates the prediction of this hazard, and climate change is expected to exacerbate extreme weather events, which present a substantial threat to economic and social advancement (Chen et al. 2024).

Figure 2.2 illustrates a river flood, or fluvial flood, which transpires when the water level in a river, lake, or stream ascends and inundates the banks, beaches, and adjacent land. Substantial precipitation or snowmelt may have contributed to the increase in water level.

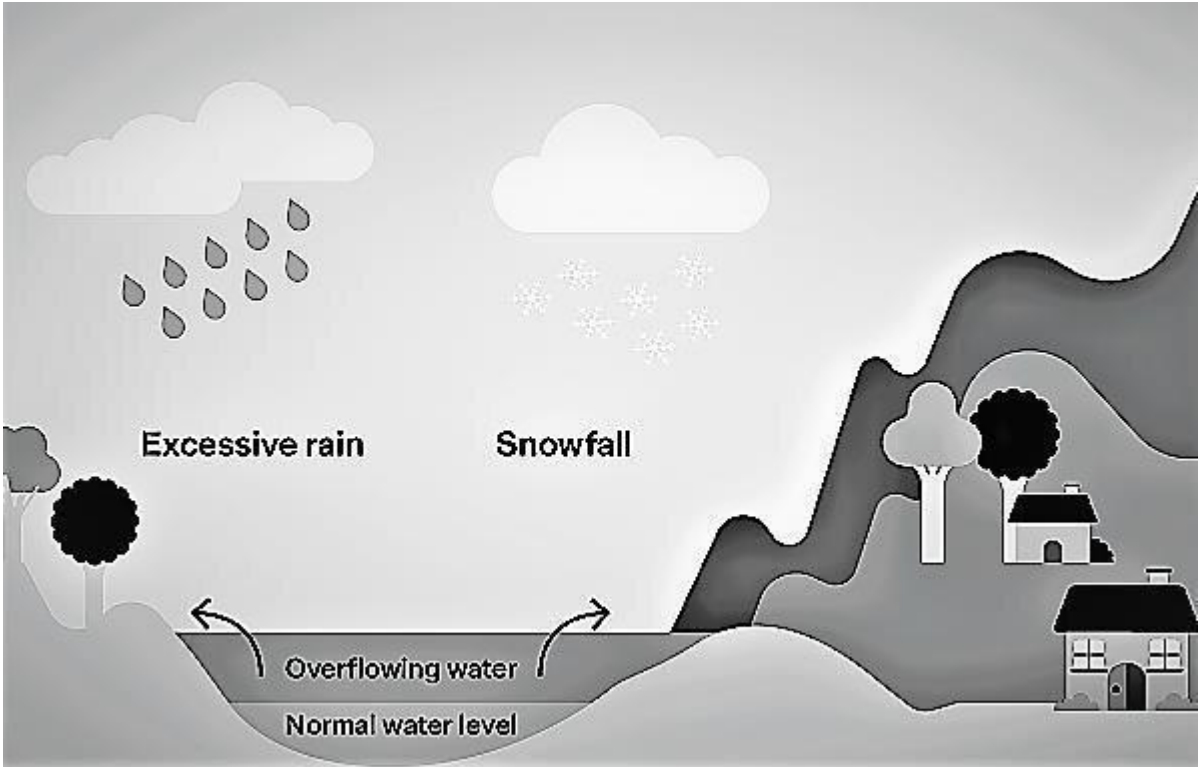


Fig.2.2. River floods (fluvial floods) (Mardaid et al. 2023)

**2.3.3 Urban flood**

Urban flooding primarily transpires in metropolitan regions, especially in flat and low-lying terrains where drainage systems are insufficient or poorly constructed, often impeded by

accumulated municipal waste or degraded soil elements. The fast urbanization and haphazard growth of cities have heightened the incidence of flooding. The conversion of natural landscapes into paved and asphalted roadways markedly elevates runoff, occasionally by a factor of six compared to natural conditions. Urbanization markedly decreases the natural water absorption capacity, frequently diminishing it by a factor of 2 to 6 relative to natural landscapes.

Urban flooding has become a critical global issue that will influence the future evolution of urban areas. Global warming has drastically modified precipitation patterns, elevating flood hazards in several urban regions. (Sim & Kim, 2024; Dwarakish et al., 2024)

Figure 2.3 shows the urban flooding of Taiyuan City.



Fig 2.3 : The scene of an urban flood in Taiwan (Sung et al., 2015)

### 2.3.4 Flash flood

Flash floods are surface runoff occurrences in mountainous watersheds resulting from brief, intense rainfall. These occurrences are marked by their abruptness, destructiveness, and swift fluctuations in surface runoff, frequently precipitating calamities such as landslides and debris

flows. The water level ascends rapidly, complicating predictions by local rapid-response teams and hence providing insufficient time to offer warnings.

Owing to the intricacies of flash flood disasters, which encompass diverse hydrological processes and nonlinearities, ambiguous disaster mechanisms, multiple influencing factors, and restricted data availability, the pivotal technological research on flash flood risk assessment remains in its nascent phase and is still undergoing exploration. (Li et al., 2024; Alarifi et al., 2022)

Figure 2.4 shows the flash flooding of Wenchuan, china.



Fig 2.4 Damage caused by flash floods in Wenchuan, china (Jin et al., 2023)

## 2.4 Flood risk in MENA region

Flooding in the MENA region is intensified by climate change, resulting in heightened migration and the emergence of environmental refugees, particularly as a consequence of severe droughts and extreme rainfall events.

Recent occurrences of extreme and frequent flash floods in the MENA arid zones have led to considerable economic and property losses. In many MENA countries, the low probability of flooding has hindered their preparedness for flood risks, resulting in a neglect of related research, which has been overshadowed by drought management efforts and their effects on water resources. In the past two decades, the region has undergone a significant change in its rainfall patterns. Numerous Arab cities, including Cairo (2020), Kuwait (2018), Riyadh (2016),

Casablanca (2016), Alexandria (2015), Doha (2015), Guelmim (2014), and Muscat (2007), have encountered flash floods, notwithstanding their predominantly arid and semi-arid climates. These events have resulted in loss of life and significant damage to properties and other urban assets. In this region, such casualties typically result from a combination of factors, including extreme precipitation, inadequate urban stormwater infrastructure and drainage systems, silting of sewers and inlets due to sandstorms, urban streams overflowing their banks, uncontrolled urban sprawl, rising groundwater tables, backwater effects from tides on drainage system outlets in coastal cities, and the steep morphology of upstream basins. (Loudyi & Kantoush, 2020; Wasimi, 2010 ; Al-Delaimy, 2020)



Fig 2.5 The affected areas by flash floods in MENA region (Kantoush et al., 2021)

## **2.5 Floods risk in Algeria**

Floods in Algeria pose a significant threat to both the inhabitants and the environment. In recent years, this risk has assumed a significant role among municipal and national authorities. Research on urban protection, wadi development, and flood risk mapping has been conducted to reduce and alleviate this hazard.

Algeria has encountered multiple flood disasters. Civil protection reports that 485 municipalities, constituting one-third of 1541, are classified as flood-prone zones with varying levels of danger. In October 1994, nationwide floods caused 60 deaths and left hundreds unaccounted for during a 10-day period of severe weather. The flood that impacted the Bab El Oued region of Algiers on 10 November 2001 resulted in a catastrophic scenario, leading to 750 fatalities, 115 individuals reported missing, and over 30,000 people rendered homeless, alongside economic damages exceeding 250 million euros. The flood transpired on 1 October 2008 in Ghardaia, southern Algeria, resulting in over 100 fatalities, 86 injuries, 4 individuals missing, and 756 families affected by the calamity. The anticipated material damage is around 40 million euros. (Hafnaoui et al., 2023; Atallah et al., 2016)

## **2.6 Flash floods risk in Algeria**

These floods (flash floods) originate from result from torrential rainfall, amounting to 3 to 12 months of precipitation occurring over a span of 3 to 7 hours. Rainwater drainage systems (sanitation networks and flood spillways) are presently inadequate to manage these types of floods. Flash floods are a somewhat obscure phenomenon that necessitates comprehensive research for accurate prediction. The most of flash floods and catastrophic floods transpire immediately following the hot season.

Floods that transpire in summer, following an extended drought or at the onset of the rainy season, frequently arise from heavy precipitation. These precipitation events produce turbid flows, significantly laden with silt (MEGNOUNIF and GHENIM, 2016). By transporting substantial volumes of mud and debris, they can entomb residences and automobiles. Erosion

and sediment deposition in the riverbed alter its morphology (Graf and Altynakar 1996), hence elevating flood risks.

No comprehensive research has been conducted on flash floods in Algeria, despite the significant damage observed in recent years in the northern region. The optimal timeframe for the occurrence of these floods was September, October, and November; however, at that time, there was no distinction made between flash flooding and gradual flooding. Furthermore, the onset of autumn instills fear in the populace due to its association with flooding. For the dam builders, it was the moment to fill the dams, however it was also the opportune time for sedimentation, as these floods discharge substantial amounts of silt. A novel climate is emerging in the Mediterranean basin today .It is characterized by an extended period of drought succeeded by a brief period of flooding. (Remini, 2023)

Table 2.1: Inventory of tragic floods in Algeria

<b>Date of the event</b>	<b>Affected areas</b>	<b>Number of victims</b>
October 12, 1971	Azzazga (W Tizi Ouzou)	40 dead
March 28 to 31, 1974	Alger et Tizi Ouzou	52 dead
September 01, 1980	EL Eulma (W.Sétif)	44 dead
August 22, 1983	Birrine ( W.Djelfa )	10 dead
February 03, 1984	Jijel, Constantine, Skikda, Guelma, Khenchla et Oum El Bouaghi	23 dead
July 05, 1987	Batna	02 dead
September 01, 1989	Biskra	02 dead
September 21, 1989	M' Sila	01 dead
October 15, 1989	Ain Defla	01 dead
June 03, 1991	Ghardaia	09 dead
January 26 - 27, 1992	Alger, Blida, Tipaza, Chlef, Ain Defla, Medea...	10 dead

October 20, 1993	Oued R'hiou (W. Relizane)	22 dead
September 23, 1994	Bordj Bou Arréridj, Msila, Djelfa, Medea, Bouira, Ain Defla et Tiaret	27 dead
September 29 to October 02, 1994	Ghardaia, Laghouat, Biskra, Mascara, Tissemsilt et <b>Sidi Bel Abbés</b>	21 dead
April 04, 1996	Annaba et El Tarf	5 dead
January 14, 1999	Adrar	12 dead
September 28, 2000	Bou Saâda (W. M'Sila)	01 dead
October 14, 2000	Ain Temochent	04 dead
October 23, 2000	Naama	05 dead
October 24, 2000	<b>Sidi Bel Abbes</b> , Tissemsilt, Chlef et Ain Defla	01 dead
November 10 and 11, 2001	Bab El Oued (Alger)	800 dead
April 18 and 19, 2007	Ghardaïa	29 dead



Fig 2.6 Flood of Ain Sefra southwest of Algeria on September 7, 2024 (by karim bouchetata, photographer)



Fig 2.7 flood damage in In Guezzam city in August 2018(Madi & Bidjaoui, 2024)

## 2.7 Flood risk in mekerra

The Mekerra basin, home to a population of 200,000 individuals, endures frequent flooding

The Upper and Central region endures recurrent and catastrophic floods, intensified by the existence of large metropolitan centers like Sidi Belabbes and Sidi Ali Benyoub. These densely populated metropolitan regions, in conjunction with rural settlements, exacerbate the risk of flooding. Between 1986 and 2009, civil protection services documented 21 floods, or almost one flood annually. The flooding incidents caused fatalities and significant property damage, encompassing agricultural and industrial losses (Abdelhalim, 2012). All floods were instigated by storms, with 12 of the 21 events transpiring between late summer and early fall. The overall recorded damages surpassed 850 displaced families and resulted in 10 fatalities (Atallah et al., 2016; Kouidri et al., 2019). Table delineates the significant floods that transpired between 1986 and 2007, which resulted in inundation in the primary communities within the Wadi Mekerra basin.

Table 2.2 : Human casualties associated with flood episodes in the Wadi Mekerra basin (1986–2007)

Date	Location	Losses	
		Dead	Homeless families
October 4, 1986	Sidi Bel Abbas	1	200
April 30, 1990	Sidi Bel Abbas	2	130
September 29, 1994	Sidi Bel Abbas	2	22
	Sidi Bel Benyoub	1	–
December 5, 1995	Sidi Bel Abbas	–	3
August 17, 1997	Moulay Slissen	1	34
September 27, 1997	Sidi Bel Abbas	1	–
December 13, 1997	Sidi Bel Abbas	1	5
July 27, 2000	Ras El Ma	–	100
October 23, 2000	Sidi Bel Abbas	1	7
	Sidi Lahcen	–	50
	Boukhanefis	–	31
	Sidi Khaled	–	50
August 2002	Throughout the province	–	200
June 8, 2003	Moulay Slissen	–	10
May 27, 2006	Ras El Ma	–	23
	Sidi Khaled	–	9
	Boukhanefis	–	5
April 2007	Moulay Slissen	–	50

## 2.8 Rainfall-Runoff Models:

Rainfall-runoff models are crucial instruments for comprehending and forecasting the hydrological reaction of a catchment to precipitation events. These models differ in complexity,

data needs, and applicability based on the study area and objectives. The primary classifications of rainfall-runoff models encompass:

**a. Conceptual models:**

Conceptual models are hydrological models that employ simplified mathematical representations of a system, utilising interconnected storages to depict various components of the hydrological process through recharge and depletion. The conceptual models are typically lumped, employing uniform parameter values across the whole watershed while disregarding the spatial diversity of watershed properties. The conceptual models heavily depend on observed data, and the outcomes are contingent upon the quality of the input data utilised in the model (Jaiswal et al., 2020). Calibrating conceptual models necessitates extensive hydro-meteorological data (Kling & Gupta, 2009). Conceptual models illustrate the water balance equation, detailing the conversion of precipitation into runoff, evapotranspiration, and subterranean water, as represented in the following equation:

$$(1) \quad P - ET - Q_s \pm GW = \frac{\Delta S}{\Delta t}$$

where,  $P$ ,  $ET$ ,  $Q_s$ ,  $GW$ , and  $\frac{\Delta S}{\Delta t}$  are precipitation, evapotranspiration, surface runoff, ground-water, and change in storage, respectively (Elizabeth et al, 2013).

Figure 2.8 illustrates a schematic representation of the tank model, a widely known conceptual model.

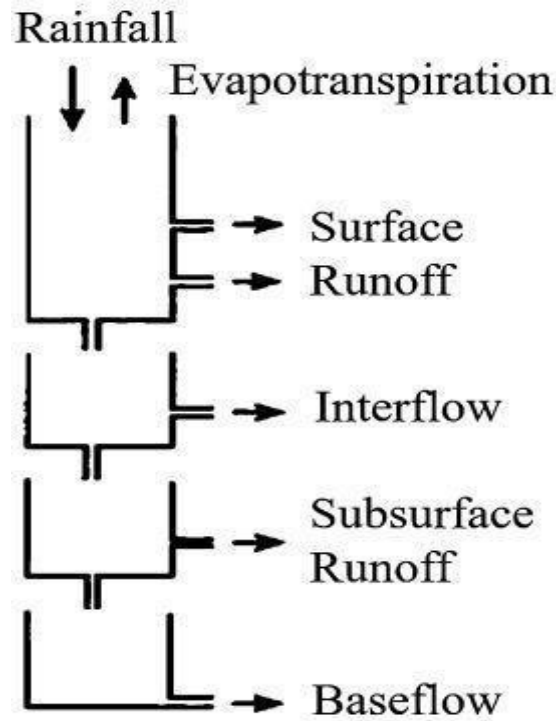


Fig 2.8 : Schematic diagram of the Tank model (Z. Liu et al., 2019).

**b. Empirical models:**

These are referred to as black-box models, which depend on previous data and statistical correlations to forecast hydrological responses. They do not necessitate a profound comprehension of the underlying processes but are efficacious for particular data-intensive circumstances. They are sometimes referred to as data-driven models, utilising non-linear statistical connections between variables and outcomes. They are focused on observation and rely significantly on the precision of input (Olaleye et al., 2024).

Empirical models are most effective when no additional outputs are necessary; for example, such models cannot ascertain the distribution of runoff between upstream and downstream regions. Empirical models yield effective modelling outcomes in ungauged watersheds due to insufficient specific knowledge regarding the watershed. Empirical models are chosen for several reasons, including as ease of implementation, rapid calculation rates, and cost-effectiveness. A drawback of empirical models is that they may produce outcomes that diverge from established theoretical analysis recommendations. The primary constraint of empirical models is that their parameters

cannot be immediately ascertained from the watershed, necessitating calibration (Jehanzaib et al., 2022b).

**c. Physical models:**

Physical process-based models are abstract mathematical representations of actual phenomena. These are referred to as mechanistic models, as they incorporate principles of physical processes. Distributed models fall under the classification of physical process-based models. In a distributed model, all hydrological phenomena, such as runoff generation, snow accumulation and melt, groundwater recharge, evapotranspiration, soil moisture dynamics, and flow in lakes and rivers, are interconnected as shown in Figure 2.14. The parameters of distributed models indicate the spatial variation of properties within the watershed and differentiate changes in the hydrologic processes occurring throughout it. Each minor component of the watershed is individually modelled to consider its hydrological connectivity with the neighbouring component (El-Nasr et al., 2005; Troutman, 1985).

Physical models, being inherently distributed, necessitate extensive topographical, soil, land use, and climatic data to establish a framework for examining alterations in the hydrological cycle resulting from human interventions and climate change for the management of water resources (J. Wang et al., 2011; Chen et al., 2015).

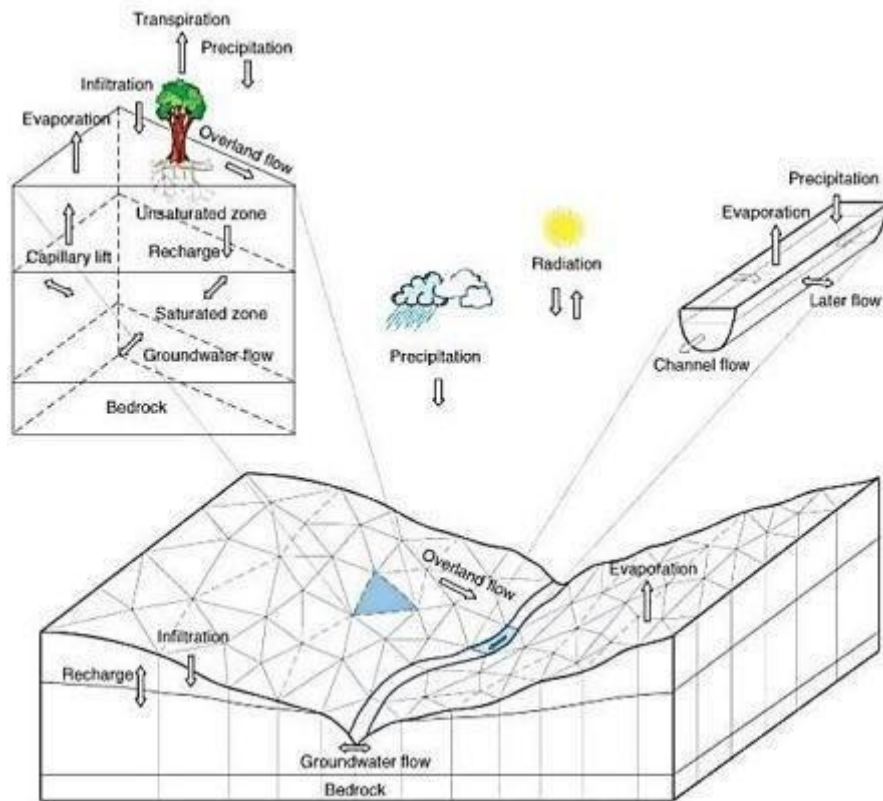


Fig 2.9: Schematic diagram of Physical model (Qu & Duffy, 2007).

Table delineates the three principal structural classifications of rainfall runoff models, accompanied by their corresponding advantages and disadvantages. (attachement)

## 2.9 Rationale for selecting physical models:

### - The necessity for comprehensive flood risk assessment:

Physical models yield intricate outputs, including high-resolution inundation maps, which are vital for flood risk assessment. They also replicate the physical processes that dictate flood dynamics, facilitating a thorough comprehension of the system.

### - The intricacy of basin:

Physical models are geographically distributed and can accommodate the intricate topography and land-use diversity. They model surface runoff, subsurface flow, and inundation processes, rendering them adept at reproducing the swift hydrological reactions characteristic of flash floods.

- **Data accessibility:**

Physical models necessitate high-resolution data, like Digital Elevation Models and land use maps. This guarantees precise depiction of the basin's hydrological dynamics and dependable model results.

- **Constraints of conceptual and empirical models:**

Although conceptual models provide a compromise between simplicity and process representation, they are deficient in the spatial detail required to accurately depict the intricate topography and land use variety. The empirical models are overly simplistic and lack a physical foundation, rendering them inadequate for reproducing the swift and intricate hydrological responses.

## **2.10 Reasons the RRI Model is the optimal selection**

- **Comprehensive simulation of precipitation, surface runoff, and flooding**

The RRI model is specifically engineered to mimic rainfall, runoff, and flood processes within a unified framework. This integrated method is especially beneficial in basins sensitive to flash flooding, necessitating a model capable of swiftly simulating the shift from precipitation to runoff and flooding.

The RRI model generates comprehensive inundation maps, essential for flood risk evaluation and management, which are often absent in numerous other physical models.

- **Spatially distributed methodology**

The RRI model is a spatially distributed framework that partitions the watershed into grid cells and simulates hydrological processes for each individual cell. This methodology is crucial due to the intricate geography of the watersheds.

The RRI model can integrate land use data to precisely depict the effects of urbanisation, agriculture, and natural vegetation on runoff generation.

- **Capability to model surface and subsurface flow**

The RRI model mimics surface runoff and subsurface flow, offering a thorough comprehension of flood dynamics. This feature is essential for the Basins situated in semi arid environment and steep slope, which result in rapid runoff generation that the RRI model can well mimic.

### **2.11 Demonstrated Efficacy in Comparable Situations**

The RRI model has been effectively utilised in multiple places with features akin to the Mekerra Basin, showcasing its dependability and precision. Illustrations comprise:

Pakistan: the RRI model was utilised during the 2010 floods, showcasing its capacity to replicate flash floods in semi-arid areas (Sayama et al., 2012).

Oman: The model was employed to simulate precipitation and runoff resulting from the intense flash floods induced by the Gonu-2007 and Phet-2010 tropical cyclones in Wadi Samail, Oman (Abdel-Fattah et al., 2018)

Brazil: The model was employed to investigate flash flood modelling and mitigation in Arid and Semiarid Basins, specifically focussing on the same basin case study in Brazil (Saber et al., 2021).

### **2.12 Previous studies**

Abbes and Meddi (2016) investigate the flooding challenges in Wadi Mekerra, highlighting the perilous flash floods that impact the town of Sidi Bel Abbès. The investigation utilizes the Muskingum model to analyze flood propagation and the QdF model for the statistical examination of flood characteristics. The Muskingum model produced unsatisfactory results for flood forecasting at the measurement station level within the basin, which is critical for calculating flood flows. Alternatively, the results demonstrate that the exponential distribution accurately represents the flood flow characteristics in this area. The subpar outcomes associated with the Muskingum method can primarily be attributed to the climatic variations between Mekerra and Ohio, the region where the method was originally formulated by engineers. This also evaluates the linearity in storage-flow relationships, which might not be applicable for rivers exhibiting significant complex geometries.

(Atallah et al., 2016) introduce a hydraulic model that employs the Runge-Kutta Discontinuous Galerkin (RKDG) finite element method for simulating flood propagation. The study also highlights important hydromorphometric and climatic factors that play a role in flooding. The model demonstrates a strong capability in predicting flood patterns with minimal input data; however, it falls short in providing spatial information regarding floods.

In their study, Lehabab-Boukezzi et al. (2016) utilize the HEC-HMS hydrological model to simulate the rainfall-runoff processes within the Mekerra watershed in Algeria, applying the GLUE method for uncertainty analysis. The results indicate that different parameter sets produced via the Monte Carlo method provide effective simulations, especially concerning hydraulic conductivity. The investigation underscores considerable ambiguities arising from various origins, stressing the necessity of integrating diverse probability assessments to improve forecasting precision.

The study by Maref and Seddini (2018) demonstrates the use of the MERCEDES distributed hydrological model to simulate flood generation in the Wadi Mekerra basin, located in northwest Algeria, which is characterized by a semi-arid climate. The model employs daily rainfall-runoff data in conjunction with spatial inputs like topography and land use to forecast runoff. The results demonstrate a promising ability to capture flood dynamics, although there is a noted tendency to underestimate peak flows. Furthermore, the sensitivity analysis indicates that the hydrological response is greatly affected by alterations in land use and the seasonal variations in vegetation cover. While the results are promising, this method might not fully account for the intricate dynamics of flooding, particularly in urban or complex environments. This method necessitates high-quality input data, including rainfall and soil properties, which may be scarce in certain locations. This method lacks the capability to deliver spatial information regarding floods, including details like water height.

Despite existing studies on floods in many forms, there remains a necessity for comprehensive research that examines all contributing elements, including topography, land utilization, and precipitation. Despite existing studies in this area, they have failed to deliver a thorough analysis of the basin and geographical data regarding floods.

### **2.13 Constraints of Alternative Physical Models**

Although various physical models, like SWAT, MIKE, and HEC-HMS, are extensively employed for flood risk evaluation, they include constraints that render them less appropriate for the Mekerra Basin:

- HEC-HMS: Primarily intended for flood forecasting and does not offer comprehensive inundation maps (Sahu et al., 2023)
- SWAT: emphasises long-term hydrological dynamics and water quality, rendering it less appropriate for flash flood modeling (Aloui et al., 2022; Tan et al., 2020)
- MIKE: necessitates substantial data and computing resources, which may be impractical for the Mekerra Basin (Hill et al., 2023)

The Rainfall-Runoff-Inundation (RRI) model is the optimal selection for flood risk evaluation in the Mekerra Basin, owing to its capacity to simulate rainfall, runoff, and inundation processes within a unified framework. Its spatially distributed methodology, adaptability, and shown efficacy in analogous scenarios render it particularly appropriate for elucidating the intricate hydrological processes within the basin. This work use the RRI model to elucidate flood dynamics and enhance flood risk management in the Mekerra Basin.

*Chapter 3:*  
Study Area

### **3.1 Introduction:**

The fundamental spatial and contextual framework for flood risk assessment in the Mekerra Basin, located in the northwest of Algeria, is established by outlining the geographical, geomorphological, and hydrological factors that influence flood dynamics in the region. A rigorous analysis of the basin's physical characteristics—such as topography, drainage patterns, and climate—complements the examination of manmade elements like land use and infrastructure, establishing an empirical foundation for understanding flood drivers and vulnerabilities. Grounding the research in local realities, this approach substantiates theoretical premises and guides focused mitigation strategies while integrating interdisciplinary perspectives from physical geography, environmental science, and risk management. Precise maps, geomorphometric indices, and hydrological data further substantiate the choice of the study area, enhancing the reproducibility and practical significance of the findings for flood resilience planning.

### **3.2 Geographical Location and Boundaries:**

The Mekerra watershed is located in the northwestern region of Algeria, roughly 400 km from the capital, Algiers (Figure 3.1). Spanning an area of about 3000 square kilometers, The watershed is situated within the longitudes of 0° 20' 34.8" W and 1° 10' 15.6" W, and the latitudes of 34° 18' 10.8" N and 35° 22' 34.8" N.

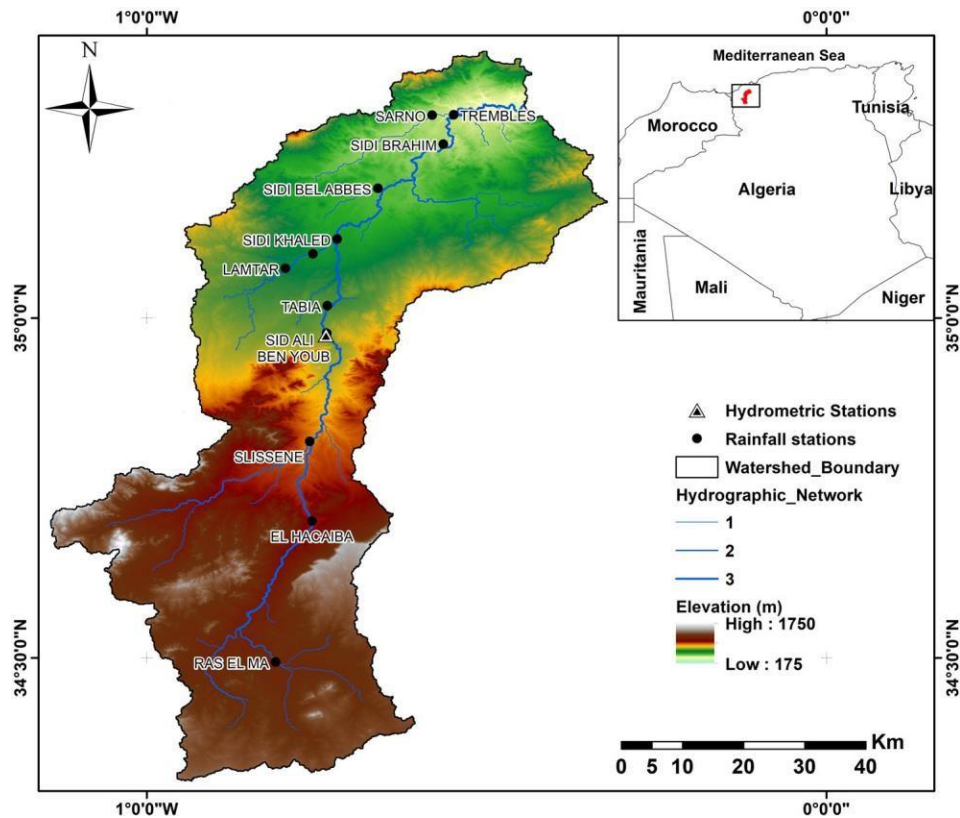


Fig 3.1: Location of Mekerra watershed

### 3.3 Geomorphological Characteristics:

Geomorphological parameters are essential for flood risk assessment, as they determine the physical dynamics of water transport across terrains. The terrain's shape, comprising slopes, valleys, and plateaus, substantially affects the velocity and direction of surface runoff during precipitation events. The characteristics of soils and sediments influence their ability to hold or transport water, affecting flood probability; for example, sandy soils often promote superior drainage relative to clay-dominated areas. The morphology of river channels, including width, depth, and meandering extent, significantly influences floodwater conveyance capacity, since confined or obstructed channels can intensify flooding conditions (Arnaud-Fassetta et al., 2009; Barrocu & Eslamian, 2022). Moreover, comprehending the dynamics of floodplains—

characterized by previous flood patterns, sediment deposition, and vegetation cover—improves projections of inundated regions. Effective flood risk management requires spatial considerations guided by geomorphological evaluations to direct land-use planning away from high-risk areas. Ultimately, the ramifications of climate change, resulting in modifications to geomorphological characteristics such as coastal erosion and changing sediment dynamics, require ongoing evaluation of flood risks to guarantee thorough preparedness methods (Cunha et al., 2017; Hooke, 2016).

Segmenting a hydrographic basin into sub-basins is an essential methodological strategy that improves flood risk assessment accuracy. This subdivision considers hydrological and geomorphological diversity, as fluctuations in precipitation patterns, soil permeability, terrain, and land use differentially affect flood formation and propagation throughout the basin. By isolating smaller, more homogeneous sub-basins flood modelling becomes more precise, as localised parameters like drainage density, channel slopes, and sediment dynamics are better represented. From a computational perspective, using sub-basins diminishes data complexity, enhancing the feasibility of hydrological simulations. This method not only enhances flood understanding but also supports spatially adaptive flood management strategies, optimizing mitigation efforts across the basin (Abdelgawad et al., 2024; Abrar et al., 2024; Awawdeh et al., 2024; Bashir & Alsalman, 2024; Wardhani et al., 2024).

To further refine flood risk assessment in the Mekerra Basin, Digital Elevation Models (DEMs) and Geographic Information Systems (GIS), are employed to analyze flow direction and stream order. This enables a detailed examination of hydrological dynamics and allows for the subdivision of the basin into ten sub-basins (Figure 3.2), allowing for a more accurate representation of local geomorphological and hydrological variations.

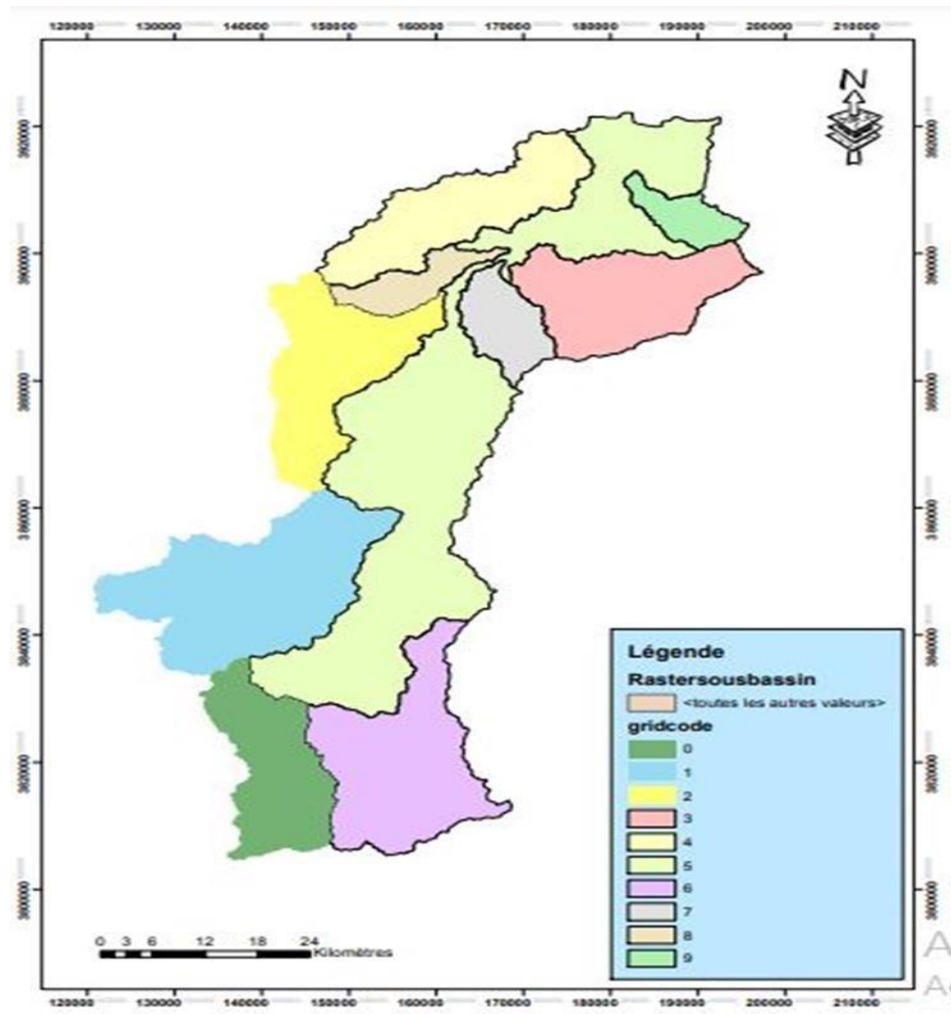


Fig 3.2: Sub-bassins of mekerra

### 3.3.1 Watershed area (A)

The watershed area represents the geographic region that directs surface water to a common outlet, such as a river, lake, or ocean. It is often referred as a drainage basin or catchment area Schumm (1956).

In morphometric analysis, the watershed area (A) is a fundamental parameter. As the area expands, the drainage network grows, increasing the number and length of streams. A larger watershed generally experiences higher cumulative rainfall, resulting in greater surface runoff and, consequently, an elevated risk of flooding. However, even smaller basins can experience severe flooding due to specific morphometric characteristics that influence water accumulation and discharge (Abdeta et al., 2020).

To compute the watershed area accurately, DEMs and GIS are utilized. DEMs provide high-resolution elevation data, allowing for the precise delineation of watershed boundaries based on topographic gradients. GIS tools facilitate hydrological analyses, enabling the extraction of the watershed area through flow direction modeling and watershed delineation techniques. These technologies improve spatial analysis accuracy, enhancing flood risk predictions.

### **3.3.2 Perimeter of the basin (Pr)**

The watershed perimeter refers to the total length of the boundary that encloses a drainage basin, distinguishing it from adjacent basins Schumm (1956). This parameter plays a crucial role in morphometric analysis, influencing hydrological characteristics such as runoff patterns and water retention capacity. A larger perimeter often indicates a more irregularly shaped watershed, which can affect flow concentration and flood response time. More compact basins tend to have shorter lag times, leading to quicker runoff and potentially increasing flood risk, while elongated or irregular basins may distribute runoff over a longer period.

To precisely compute the watershed perimeter, DEMs and GIS tools are employed. DEMs provide topographic data, enabling the accurate delineation of watershed boundaries, while GIS spatial analysis techniques allow for the tracing and measurement of perimeters through contour extraction and hydrological feature mapping. Automated GIS functions ensure precision and efficiency in perimeter calculation, enhancing watershed characterization for flood risk assessment. The Mekerra sub-basins perimeter range between 51 km and 405 km, highlighting the variability in basin shapes.

### **3.3.3 Stream frequency (Sf)**

Stream frequency is a key metric in hydrological studies, signifying the quantity of stream segments per unit area within a watershed. It is calculated using the formula:

$$(2) \dots \dots \dots Sf = \frac{N_U}{A}$$

where:

*Sf* is the Stream frequency

*N<sub>U</sub>* : The total number of streams

*A* : the Basin area

This measure serves as a valuable indicator of the complexity of the drainage network and has significant implications for runoff dynamics. Higher stream frequency values suggest a more intricate drainage system, which can lead to accelerated surface runoff during precipitation events. Basins with numerous streams generally collect and channel water more efficiently, increasing the likelihood of flash flooding. This makes stream frequency analysis a crucial component of flood risk assessments (Farhan et al., 2016). For the **sub-basins of the Mekerra Basin**, the computed **stream frequency values (Sf)** are reported in **Table 3.1**.

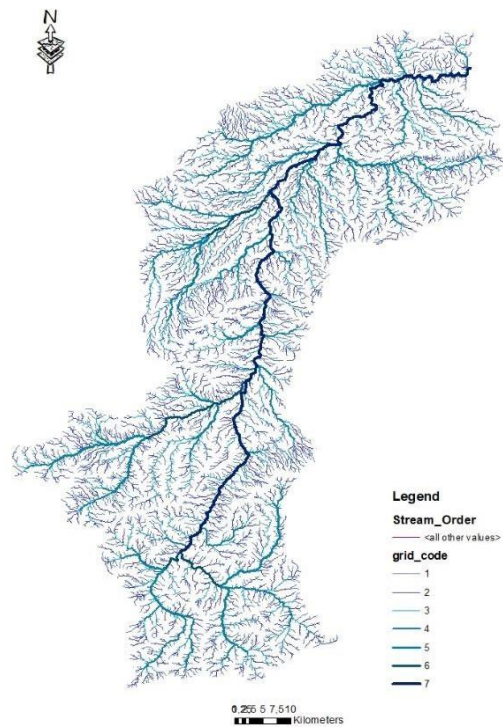


Fig 3.3: Stream order of mekerra

### 3.3.4 Drainage density (Dd)

Drainage density is a crucial metric of the linear scale of landforms in stream-eroded topography.

It is defined as the ratio of the total length of streams of all orders inside a basin to the basin's area, expressed in km/km (Horton, 1932):

$$(3) \dots \dots \dots Dd = \frac{L_U}{A}$$

where:

*Dd* : Drainage density (km/km<sup>2</sup>)

*L<sub>U</sub>* : Length of all streams within the basin (km)

*A* : Basin area (km<sup>2</sup>)

The drainage density reflects the proximity of channel spacing, hence offering a quantitative assessment of the average stream channel length across the entire basin. Additionally, it provides insight into the physical features of the underlying rocks.

Low drainage density is found in areas with highly resistant and permeable subsoil, characterized by dense vegetation and low relief, while high drainage density is common in places with weak, impermeable subsurface materials, sparse vegetation, and high relief (Gajbhiye et al., 2013b).

Drainage density (Dd) denotes the distribution and configuration of the drainage network within the basin area. Elevated drainage density correlates with heightened flood peaks, while diminished drainage density results in reduced flood levels. A high drainage density indicates impermeable soil, steep slopes, elevated surface runoff, and less infiltration, resulting in a significant possibility for flooding, and conversely (Obeidat et al., 2021).

For the sub-basins of the Mekerra Basin, the computed drainage density Dd values are reported in Table 3.1.

### 3.3.5 Inverse shape form (Ish)

The inverse shape form is a dimensionless morphometric parameters that measures the elongation or linearity of a drainage basin by relating its area to the square of its maximum length (Horton, 1945). Unlike the compactness index, which assesses circularity, Ish specifically analyzes the elongation or narrowness of a basin, directly influencing hydrological behavior and flood dynamics. It is computed using the following formula:

$$(4) \dots \dots \dots Ish = \frac{L^2}{A}$$

where:

*Ish*: Inverse shape form (dimensionless)

L : Maximum basin length (km)

A : Basin area (km<sup>2</sup>)

A higher Ish value indicates an elongated basin, which generally leads to a longer concentration time and delayed flood peaks, reducing flood intensity. Conversely, a lower Ish value signifies a more compact basin, where runoff is quickly concentrated, increasing the risk of rapid flooding following precipitation events.

Hydrological implications of Ish:

- Elongated basins (high Ish values) → Slower runoff concentration, lower peak discharge, longer flood duration.
- Compact basins (low Ish values) → Faster runoff response, higher peak discharge, shorter flood duration.

For the sub-basins of the Mekerra Basin, the computed inverse shape form Ish values are reported in Table 3.1.

### 3.3.6 Relief ratio (Rr)

The relief ratio (Rr) is a dimensionless morphometric parameter that measures the steepness and elevation gradient of a drainage basin by comparing its total relief (the elevation difference between the highest and lowest locations) to its maximum horizontal length (Lindsay & Seibert, 2012). It is computed using the following formula:

$$(5) \dots\dots\dots Rr = \frac{H}{L}$$

where:

Rr : Relief Ratio (dimensionless)

H : Total basin relief (maximum elevation – minimum elevation) (m)

L : Maximum basin length (km)

This parameter provides critical insights into the **basin’s potential energy for erosion and runoff production**.

- Higher Rr values → Steeper slopes, increased erosion, higher runoff velocity, and greater flood risk.
- Lower Rr values → Reduced flooding potential, as gentler slopes lead to slower runoff concentration and higher infiltration rates.

For the sub-basins of the Mekerra Basin, the computed Relief Ratio Rr values are reported in Table 3.1.

### 3.3.7 Ruggedness number (Rn)

The Ruggedness Number, also known as the basin Ruggedness Number or Topographic Ruggedness Index, is a dimensionless geomorphological metric that measures the steepness and roughness of a drainage basin's terrain. It is a critical metric for assessing hydrological and geomorphological dynamics, as it directly correlates drainage density with maximum basin relief, reflecting the structural complexity of the landscape (Adhikari, 2020).

The ruggedness number is computed using the following formula:

$$(6) \dots\dots\dots Rn = Dd * H$$

where:

Rn : Ruggedness Number (dimensionless)

Dd : Drainage Density (km/km<sup>2</sup>)

H : Maximum Basin Relief (m)

A higher **ruggedness number (Rn)** indicates a more irregular and dissected terrain, which can influence hydrological responses such as runoff velocity and erosion potential. In contrast, lower values suggest more uniform and gently sloping basin morphology. For the **Mekerra Basin**, the **Ruggedness Number, Rn, values range between 0.69 and 3.53**, highlights significant variations in topographic relief and drainage density across different sub-basins. The detailed values for the sub-basins are reported in Table 3.1.

### 3.3.8 Texture ratio (Tr)

The texture ratio is a quantitative geomorphological metric that measures ~~quantifies~~ the density of stream networks within a drainage basin in relation to its size and topographic configuration. It is a crucial parameter in assessing drainage development, as it depends on various natural factors, including climate, precipitation, vegetation, lithology, soil composition, infiltration capacity, topography, and the basin's developmental stage (Waikar & Nilawar, 2014).

The texture ratio is calculated using the following formula:

$$(7) \dots\dots\dots Tr = Nu * Pr$$

where:

Tr : Texture Ratio (dimensionless)

Nu : Total Number of Streams

Pr : Basin Perimeter (km)

A higher texture ratio signifies a denser and more intricate drainage network, characterized by a greater frequency of streams, which can result in faster runoff and increased flood susceptibility. Conversely, a lower texture ratio suggests a sparser drainage network, indicating reduced runoff concentration and a lower risk of flash flooding.

For the Mekerra Basin, the Texture Ratio,  $Tr$ , ranges between 4.09 and 13.84, highlighting spatial variations in drainage density and terrain characteristics across different sub-basins. The specific values for each sub-basin are reported in Table 3.1.

### **3.3.9 Compactness index ( $K_g$ )**

The compactness index, or circularity ratio, is a dimensionless geomorphometric statistic used to assess the shape of a drainage basin by comparing its area to that of a perfect circle with an equivalent perimeter. This denotes the extent to which a basin's configuration approximates a circle, affecting hydrological behavior and flood risk (Rai et al., 2014).

The compactness index is influenced by several factors, including the duration and frequency of streams, geological formations, land utilization and coverage, climate, topography, and gradient of the basin (Gajbhiye et al., 2013).

$K_g = 1$ : The basin is entirely circular (uncommon in nature), indicating consistent water flow concentration and reduced peak flow durations.

$K_g > 1$ : The basin is either elongated or irregular, resulting in a delayed peak discharge and less flood risk, however extended runoff duration.

$K_g < 1$ : Theoretically implausible, as a complete circle represents the most compact configuration.

For the Mekerra Basin, the Compactness Index,  $K_g$ , for the sub-basin of the Mekerra basin are reported in Table 3.1

**Table 3.1: Morphometric parameters**

	Morphometric parameter of Sb												
	Pr	A	Kg	L	Lu	Dd	He	Le	Sf	Tr	Ish	Rn	Rr
<b>Sb0</b>	106.0	281.4	1.77	26.8	10.5	2.80	1358	1048	3.0	7.99	0.5	0.87	1.2
<b>Sb1</b>	132.7	533.6	1.61	31.2	17.1	3.09	1712	802	3.44	13.8 4	0.7	2.81	3.0
<b>Sb2</b>	128.4	343.3	1.94	33.6	10.2	2.72	1188	509	3	8.02	0.39	1.85	2.0
<b>Sb3</b>	97.9	321.4	1.53	26.0	12.3	2.85	908	451	3.08	10.1 0	0.60	1.30	1.8
<b>Sb4</b>	114.9	310	1.83	35.0	8.8	2.93	1021	378	3.07	8.29	0.32	1.89	1.9
<b>Sb5</b>	405.4	1165.9	3.32	95.6	12.2	2.98	1467	283	3.06	8.79	0.16	3.53	1.2
<b>Sb6</b>	139.6	428.1	1.89	28.5	15.0	2.76	1438	1048	2.97	9.10	0.67	1.07	1.4
<b>Sb7</b>	62.0	123.8	1.56	17.4	7.1	2.68	890	475	3.03	6.04	0.52	1.11	2.4
<b>Sb8</b>	66.1	91.8	1.93	19.3	4.8	2.60	731	467	2.95	4.09	0.31	0.69	1.4
<b>Sb9</b>	51.1	77.3	1.63	14.6	5.3	2.98	765	345	3.20	4.83	0.46	1.25	2.9

### 3.4 Climate and Meteorological Conditions

The Wadi Mekerra basin is characterized by a Mediterranean climate with semi-arid tendencies, characterized sporadic, intense, and unpredictable, rainfall events (Seltzer, 1976). This climate type encompasses the northern region of Africa, which includes Algeria. The climate is distinguished by hot, dry summers with very little rainfall, and a winter that is pleasant and rainy (Djellouli, 1990).

The Mediterranean climate is characterized by a cyclogenetic setting that is notable for its brief but intense periods of rainfall (Menad, 2012).

The mean annual precipitation in the Oued Mekerra watershed ranges from 198 mm to 311 mm. The distribution of rainfall varies based on the proximity to the sea, with the northern section of

the basin receiving a higher amount of precipitation (311 mm) compared to the southern part (198 mm). Additionally, it is distinguished by a pronounced interannual variability, characterized by alternating wet and dry cycles. In arid years, the yearly precipitation might plummet to less than 50 to 80% of the average annual rainfall, intensifying water scarcity and affecting hydrological balance.

The mean annual air temperature is approximately 15°C (Atallah, 2018). August is the warmest month, with a high temperature of 40°C. February is the coldest month, with a low temperature of 0°C. The temperature exhibits a gradual decline from September to January, followed by a progressive increase until August (Mokadmi, 2012).

### **3.5 Hydrological Characteristics**

#### **3.5.1 Hydrographic network :**

The hydrographic network encompasses all natural or artificial, permanent or temporary systems that contribute to surface runoff and drainage within the basin. The hydrographic network represents one of the most significant morphological and hydrological features of the basin.

The Mekerra Wadi's hydrological course is shaped by the existing topography, evolving as it traverses the southwest-to-northeast orientation of the Tessala Mountains.

The Mekerra occupies an area of roughly 3000 km<sup>2</sup>, extending over a thalweg of about 170 km, from the elevated valleys of the steppe south of Ras El Ma to the town of Sidi Bel Abbès. The hydrographic network consists of multiple tributaries, sometimes shown as ephemeral watercourses, with the wadi mostly sustained by precipitation.

### **3.6 Land Use and Land Cover**

The Mekerra Basin exhibits diverse landscapes with distinct land use and land covers (LULC) patterns. North areas are predominantly agricultural, benefiting from relative higher precipitation and fertile soils. Urban centers are scattered throughout the basin, with Sidi Bel Abbès being the largest and most densely populated settlement. The Southern regions are characterized by arid,

barren, and unproductive lands, with limited vegetation and minimal agricultural activity due to low precipitation and poor soil fertility.

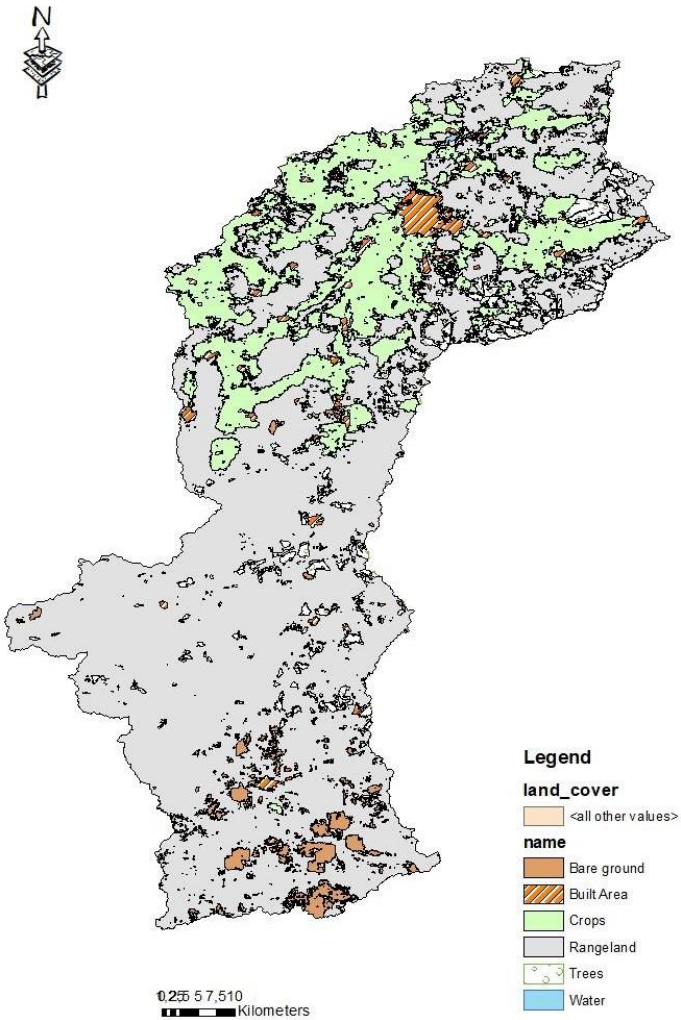


Fig 3.4: Land cover of mekerra

**3.7 Soil Types and Characteristics:**

The Mekerra wadi watershed has Quaternary and Plio-Quaternary rocks predominantly composed of alluvium and conglomerates. The region is characterzdz by Humiferous calcareous soils, which are widely distributed across the basin (Figure 3.5). The calcareous crust is porous, playing a crucial role in water infiltration and retention, particularly during flood events. The northern section of the basin exhibits significantly greater permeability than the southern section,

where infiltration capacity is significantly lower. A surface contact exists with the conglomerate channel that encompasses the water table. Beyond the dominant humiferous calcareous soils, the basin also contains calcareous soils, calcic soils, and alluvial deposits. In areas experiencing intense runoff, the underlying bedrock is exposed due to erosion (Cherif et al., 2009).

The Mekerra Basin is structurally influenced by three major faults:

- The first fault extends from the southwest to the central part of the basin.
- The second and third faults follow a west-to-east orientation.
- These faults intersect near Sidi Ali Ben Youb, contributing to local geological complexity.

These three faults significantly contribute to alleviating flood impacts by diminishing the peak flow that is released.

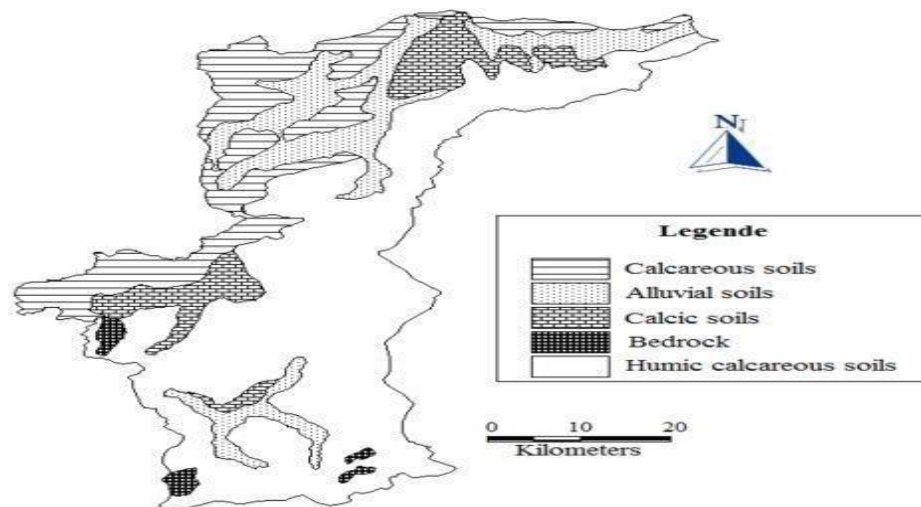


Fig 3.5: soil types map of the Mekerra watershed.

### **3.8 CONCLUSION:**

This chapter offers a comprehensive overview of the research area, encompassing its geographical and hydrological characteristics, which are crucial for comprehending the flood risk dynamics in the region.

The Mekerra Wadi exhibits significant variability in terms of morphological characteristics, climate, and even land use and soil types. These variations contribute to the complexity of flood behavior within the basin, necessitating the use of advanced modeling techniques that integrate all these factors.

This context will facilitate a more precise and focused flood risk evaluation. This information will be a vital reference for applying RRI in evaluating flood risks and formulating suitable mitigation plans.

Building on this groundwork, the subsequent chapters will employ the RRI model to analyze flood risks in the study area, offering insights into flood dynamics and guiding risk management efforts.

*Chapter4:*  
Methodology

## **4.1 Introduction**

This chapter delineates the systematic strategy employed to evaluate flood risk in Mekerra Basin utilizing the Rainfall-Runoff-Inundation (RRI) model. This physically-based, distributed hydrological model was chosen for its proven capacity to simulate integrated rainfall-runoff processes and flood inundation dynamics in semi-arid regions. The methodology incorporates multi-source data, such as high-resolution topographic data, land use/cover maps, historical precipitation records, and soil properties, to parameterize the model. A stringent calibration and validation process utilizes recorded flood events to guarantee model dependability. Subsequent flood hazard mapping integrates extreme precipitation scenarios to assess regional distributions of flood risk under existing and anticipated climatic conditions. The analytical framework tackles significant issues of data scarcity and hydrological complexity inherent to semi-arid basins, while offering a transportable strategy for flood risk assessment in analogous areas. This thorough methodology facilitates the study's aims of enhancing flood modeling methodologies and guiding risk mitigation initiatives for the Mekerra Basin.

## **4.2 Data collection**

### **4.2.1 Rainfall and Runoff Data**

The National Agency of Hydraulic Resources (ANRH) conducted the rainfall measurements, overseeing gauging stations and hydrometric assessments in Algeria. The research employed daily data gathered from 12 rainfall gauge stations for the period 1975–2003, strategically located throughout the watershed to monitor the specified flood events. Rainfall data from these gauges were interpolated throughout the watershed with the Thiessen polygon method for incorporation into the RRI model, as advised in the product's handbook.

Only data from the Sidi Ali Benyoub gauging station were utilised for the sensitivity analysis. The calibration and validation of the RRI model were predicated on two notable flood occurrences that transpired in October 1986 and September 1994. These Two events were chosen based on the availability of runoff data, so facilitating precise calibration and validation of the model. This emphasis on the events enabled the model to accurately capture the rainfall-runoff dynamics and depict the peak flood features during these intervals.

#### 4.2.2 Topographic and Watershed Data

The topographic data for this investigation were obtained from HydroSHEDS, encompassing its flow direction and flow accumulation products. These information were crucial for identifying stream networks and determining watershed borders with Geographic Information Systems (GIS). The data were analysed at a 30-second resolution, yielding a precise and comprehensive depiction of the terrain. The input data were created according to the technique specified in the RRI model manual, which involves delineating the target river basin and modifying the digital elevation model (DEM) and flow direction information to ensure compliance with hydrological modelling. This preparation guaranteed the data's appropriateness and dependability for the study aims.

The HydroSHEDS dataset was selected for this study due to its comprehensive and globally consistent representation of river basins, a feature that is essential for the effective application of the Rainfall–Runoff–Inundation (RRI) model. A comparative evaluation was performed between flow direction, flow accumulation, and slope layers generated from the HydroSHEDS product and those derived from the 30-meter Shuttle Radar Topography Mission (SRTM) data. The comparison revealed no significant deviations in the delineation of primary valley flow paths, thereby confirming the suitability and reliability of the HydroSHEDS dataset for hydrological modeling in the Mekerra Basin.

Moreover, the HydroSHEDS dataset constitutes a practical and computationally efficient choice for the RRI model, which is inherently demanding in terms of processing resources. Its standardized structure and pre-processed attributes substantially streamline model setup and execution, reducing the overall computational burden. The adoption of HydroSHEDS data is well established within the hydrological modeling community, having been successfully implemented in various regional flood studies, including those conducted in Sri Lanka, Myanmar, Thailand, and Oman (Abdel-Fattah et al., 2018; Herath et al., 2023; San et al., 2020; Sriariyawat et al., 2022).

### **4.2.3 Land use**

This study's analysis employed land use data obtained from Landsat imagery, specifically Landsat 5 Thematic Mapper (TM) data, for the historical mapping of land use in 1986. The terrain types were classified into three distinct categories (crops, rocks, and constructed places), each possessing unique water-holding capacities, a critical parameter in the RRI model. In arid climates, substantial precipitation over impermeable or clay soils can lead to an increase in runoff. The absence of vegetation and diminished soil absorption in flat terrains intensify the swift accumulation of water, heightening the flood danger. The swift proliferation of metropolitan regions and alterations in land cover convert numerous soils into impermeable surfaces, hence reducing soil infiltration capacity and augmenting runoff.

The 1986 Landsat Thematic Mapper (TM) dataset was selected for this study to establish baseline land use conditions for hydrological modeling. A comparative assessment between the 1986 Landsat TM imagery and the Food and Agriculture Organization (FAO) land use map for autumn 2024 (Fig. 3.4) indicates minimal variation in urban development across the Mekerra Basin over this period. Urbanized areas represent only a small fraction of the total basin surface, with the principal urban center, Sidi Bel Abbès, located downstream and spatially isolated from the main flood-generating zones of the Wadi Mekerra. This spatial separation implies that urban expansion within the basin exerts negligible influence on upstream flood generation processes. Furthermore, because vegetation cover in autumn is generally reduced following the summer dry season, the 1986 dataset offers a representative and historically consistent depiction of surface conditions relevant for the accurate parameterization of the hydrological model.

## **4.3 Modeling**

### **4.3.1 ArcGIS**

ArcGIS Desktop 10.8 was utilized for data processing into formats compatible with the Rainfall Runoff Inundation (RRI) Model.

### **4.3.2 Rainfall-Runoff Inundation Model**

RRI\_1\_4\_2\_6 was employed to concurrently simulate flood inundation and rainfall runoff. This approach comprises two interfaces: Command User Interface (CUI) and Graphical User Interface (GUI). This research utilized the graphical user interface.

#### **4.3.2.1 RRI Model Description**

The employed model is the 2D Rainfall-Runoff-Inundation (RRI) model, which can simultaneously simulate rainfall-runoff and flood inundation (Sayama et al., 2012). Figure 4.1 illustrates a schematic representation of the RRI model. The model addresses slopes and river channels independently. Lateral flows are modeled on slope cells in a two-dimensional framework, where a river channel is situated within a grid cell, and the model presumes that both the slope and the river occupy the same grid cell.

The model posits that both the slope and the river channel are situated within the same grid cell. The channel is represented as a singular line along the central axis of the overlaying slope grid cell. The flow in the slope grid cells is computed using the 2D diffusive wave model, whereas the channel flow is determined using the 1D diffusive wave model. The RRI model enhances representations of rainfall-runoff-inundation processes by simulating lateral subsurface flow, vertical infiltration flow, and surface flow. Lateral subsurface flow, particularly significant in hilly areas, is analyzed through the discharge-hydraulic gradient connection, incorporating both saturated subsurface and surface fluxes. The vertical infiltration flow is evaluated utilizing the Green-Ampt model. The interaction of flow between the river channel and slope is assessed using several overflow formulas, contingent upon water level and levee height circumstances.

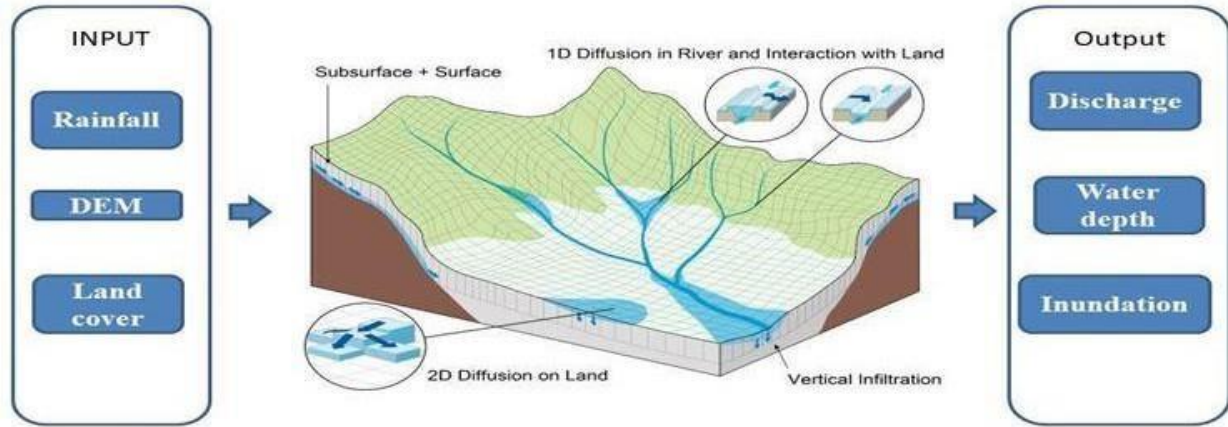


Fig 4.1: diagram of Rainfall Runoff Inundation (RRI) Model

The 1D RRI wave model is utilized for river routing calculations, whereas the 2D RRI diffuse wave model assists in determining water profile slopes. The model use the following mass balance equation:

$$\begin{aligned}
 (8) \dots\dots\dots \frac{\partial h}{\partial t} + \frac{\partial q_x}{\partial x} + \frac{\partial q_y}{\partial y} &= r - f \\
 (9) \dots\dots \frac{\partial q_x}{\partial t} + \frac{\partial(uq_x)}{\partial x} + \frac{\partial(vq_x)}{\partial y} &= -gh \frac{\partial H}{\partial x} - \frac{\tau_x}{\rho_w} \\
 (10) \dots\dots \frac{\partial q_y}{\partial t} + \frac{\partial(uq_y)}{\partial x} + \frac{\partial(vq_y)}{\partial y} &= -gh \frac{\partial H}{\partial y} - \frac{\tau_y}{\rho_w}
 \end{aligned}$$

In this context,  $h$  represents the height of water above the local surface,  $q_x$  and  $q_y$  denote the unit width discharges in the  $x$  and  $y$  directions, respectively.  $u$  and  $v$  signify the flow velocities in the  $x$  and  $y$  directions,  $r$  indicates the rainfall intensity,  $f$  refers to the infiltration rate,  $H$  is the height of water above the datum,  $\rho_w$  is the density of water,  $g$  is the acceleration due to gravity, and  $\tau_x$  and  $\tau_y$  are the shear stresses in the  $x$  and  $y$  directions.

A one-dimensional diffusive wave model is utilized for river grid cells. The geometry is presumed to be rectangular, characterized by width  $W$ , depth  $D$ , and embankment height  $H_e$ . In

the absence of accurate geometric data, the breadth and depth are estimated using the following function of the upstream contributing area  $A$  [ $\text{km}^2$ ].

$$(11) \dots\dots\dots W = C_w A^{S_w}.$$

$$(12) \dots\dots\dots D = C_d A^{S_d}.$$

In this context, the variables  $D$ ,  $W$ ,  $A$ ,  $C_d$ ,  $S_d$ ,  $C_w$ , and  $S_w$  represent the depth (in meters), width (in meters), area (in square kilometers), depth parameters, and width parameters, respectively

**4.3.2.2 RRI Model Input and Set-Up**

The model necessitated input data including satellite-derived precipitation data, topographic information, and river cross-sectional data. It integrates diffusive wave flow equations within a land surface model to address water and energy budget processes, land-vegetation-atmosphere interactions, soil moisture dynamics, and lateral water flows. Parameter calibration is executed by statistical indices and comparison with observed discharge data, whereas model validation employs river discharge data, satellite inundation extents, and additional observable data (Nastiti et al., 2015; Nastiti et al., 2018; Rasmy et al., 2019; Yao et al., 2021; Sayama et al., 2019)

Figure 4.2 shows the configuration procedure of the RRI model

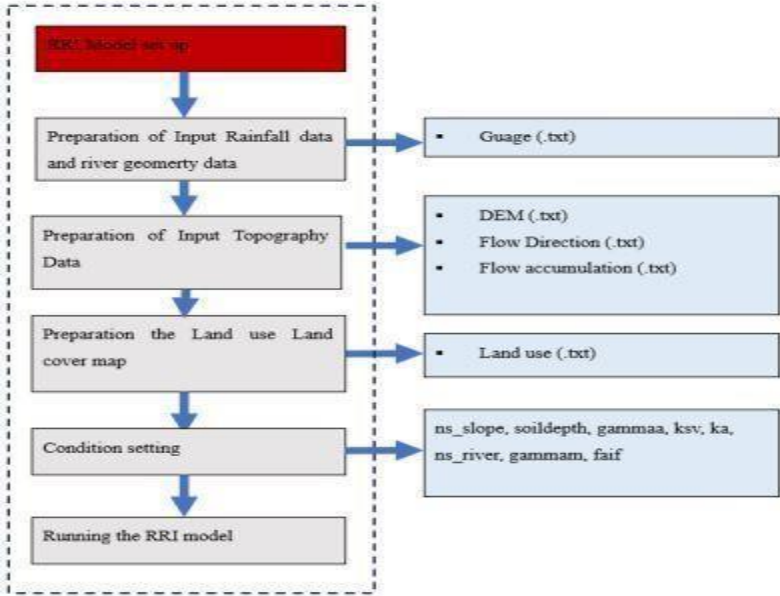


Fig 4.2: Flowchart illustrating the configuration procedure of the RRI model

## 1. Preparation of input rainfall data

The measured precipitation data were utilized for the simulated period. The recorded rainfall data were organized in an Excel spreadsheet in the following format. The data were subsequently duplicated and stored as a text file.

Figure 4.3 shows Methods for preparing rainfall data for entry into the RRI model

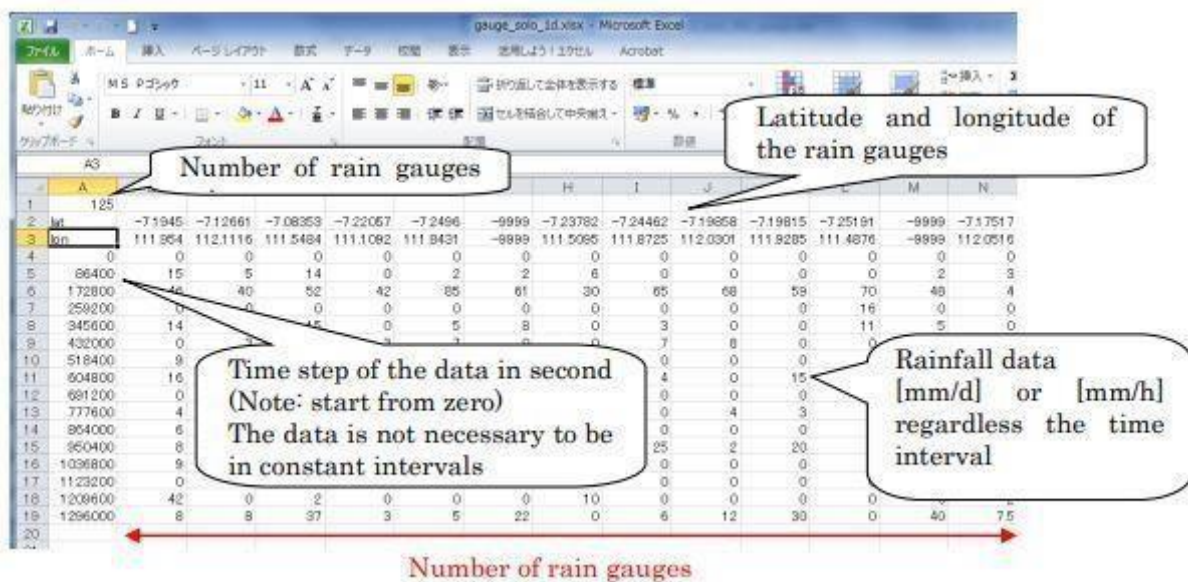


Fig 4.3: Methods for preparing rainfall data for entry into the RRI model.

## 2. Preparation of topographic data

The downloaded Digital Elevation Model (DEM) was integrated into the ArcGIS environment. A point shapefile was generated to specify the catchment outlet, which facilitated the delineation of the target catchment in conjunction with the flow direction. The DEM, flow direction, and flow accumulation were subsequently retrieved utilising the catchment raster (see to Figure 4.4-4.6). The files had been converted to ASCII format compatible with the RRI model, maintaining a comparable number of rows, columns, and cell sizes. The RRI\_Input.txt file was subsequently modified to identify the directory containing the topographic data. The RRI\_Input.exe file was executed.

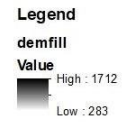


Fig 4.4 : DEM mekerra

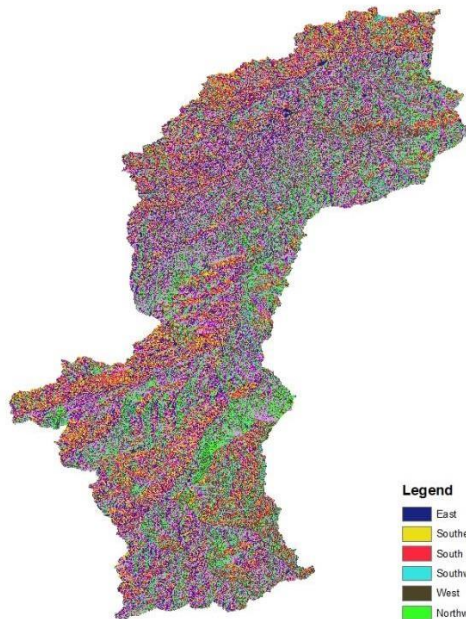


Fig 4.5: Flow direction mekerra



Fig 4.6: Flow accumulation mekerra

### 3. Preparation of the land use

This study's analysis employed land use data obtained from Landsat imagery, specifically utilising Landsat 5 Thematic Mapper (TM) data for the historical mapping of land use in 1986. The terrain types were classified into three distinct categories: crops, rocks, and built places, each possessing unique water-holding capacities, a critical parameter in the RRI model.

The polygon and clip commands were employed to extract the research catchment area, which was subsequently reprojected to align with the digital elevation model (DEM), flow accumulation, and flow direction.

The resultant raster file was subsequently transformed to ASCII format (figure 4.7) for compatibility with RRI.



Model validation follows a similar protocol, comparing simulated and observed hydrographs for the 1994 event. If validation performance is found to be strong, the model is considered robust and subsequently approved for operational use within the study. However, if validation results are inadequate, further refinement of model parameters is undertaken until satisfactory performance is attained. This iterative methodological structure ensures that both calibration and validation phases are rigorously addressed, enhancing the reliability and scientific validity of the RRI modeling approach for flood risk assessment in the Mekerra Basin.

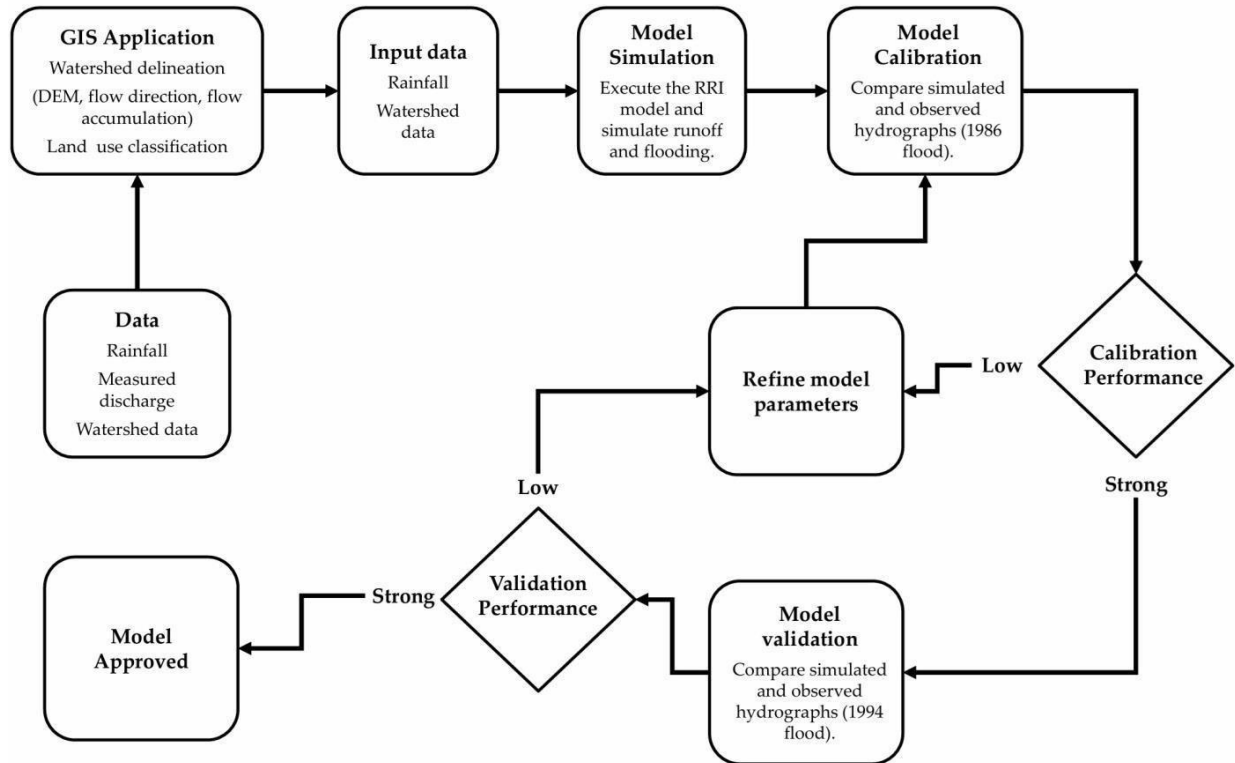


**Fig 4.8 :** Flow diagram illustrating the methodology for applying the Rainfall–Runoff–Inundation (RRI) model in the Mekerra Basin study.

#### 4.3.2.4 calibration and validation

This part employed statistical criteria for model calibration and validation. Calibration is the process of refining a model by optimising its parameters through adjustments to the model structures and boundary conditions, as well as enhancing the hydrometeorological data input (sidi ali benyoub ). The parameter value is optimised manually and qualitatively assessed, for instance, by graphing the observed and simulated discharges. The purpose of the calibration is to modify specific model parameters to reduce the discrepancy between observed and simulated discharges.

Model validation is the process of assessing the model's capacity to replicate observed data, distinct from that utilised for calibration, with acceptable precision. Throughout this procedure, calibrated model parameter values remain unchanged. The quantitative assessment of the match is the extent of deviation between the calculated and observed hydrographs (San et al., 2020b).

Figure 4.9 shows the program interface and where values are changed during the calibration and validation process.

The models are validated for two distinct flood events occurring in 1986 and 1994.

The selection of the two flood events of 1986 and 1994 for the calibration and validation of the Rainfall–Runoff–Inundation (RRI) model was a deliberate methodological decision dictated by the scarcity of complete and reliable historical flood records for the Mekerra Basin. These events represent the most comprehensively documented cases available, with data of sufficient temporal and spatial resolution to support accurate model configuration and assessment. While it is acknowledged that the inclusion of a greater number of flood events could enhance the evaluation of model robustness, such limitations are characteristic of semi-arid regions where hydrological observation networks remain sparse and discontinuous. Employing a limited dataset for calibration and validation is, therefore, an established and scientifically accepted practice in hydrological modeling, particularly within data-scarce environments. Moreover, numerous studies utilizing the RRI model in diverse geographical contexts have adopted a similar approach, prioritizing the establishment of the model’s core reliability prior to its application across multiple events. This strategy provides a scientifically sound preliminary evaluation of model performance and lays a rigorous foundation for future studies as additional hydrometeorological data become available.

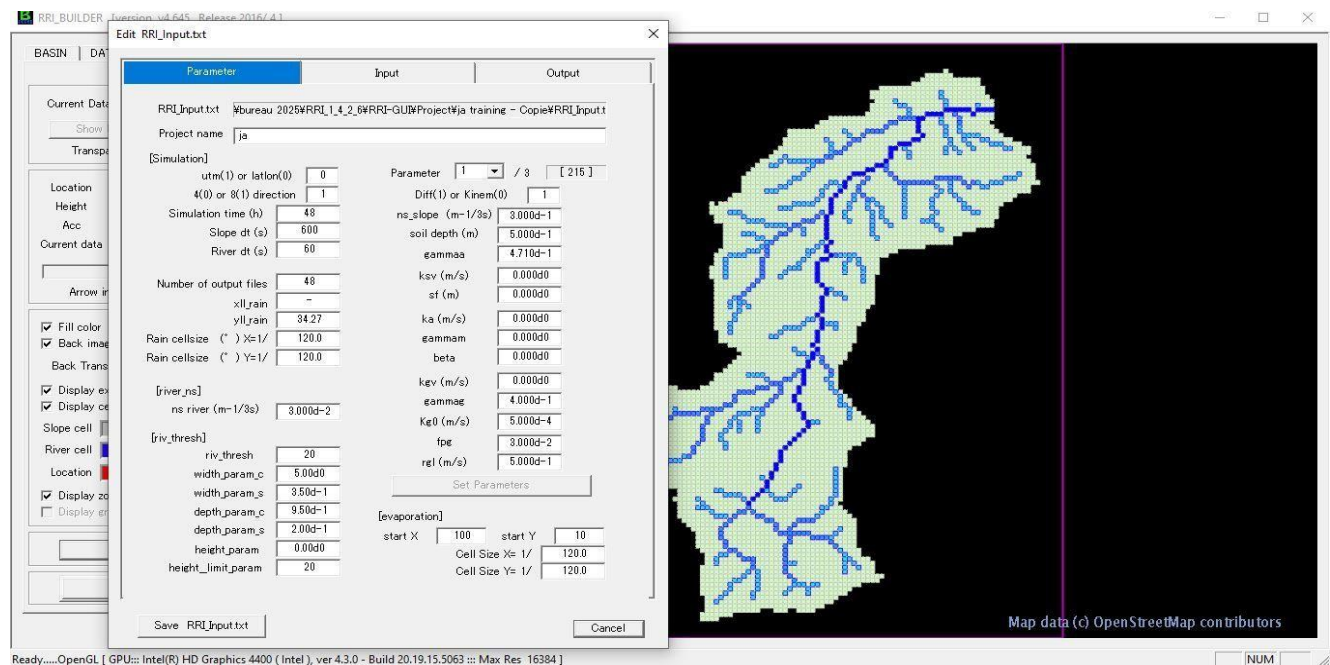


**Fig 4.9** the program interface and where values are changed during the calibration and validation process

Throughout both the calibration and validation phases, the degree of accuracy of fit between the simulated and observed runoff was assessed using the Correlation Coefficient,  $r^2$ , PBIAS, and NSE.

$$(13) \dots \mathcal{CC} = \left[ \frac{\sum_{i=1}^n (Q_{obs} - \overline{Q_{obs}})(Q_{sim} - \overline{Q_{sim}})}{\sqrt{\sum_{i=1}^n (Q_{obs} - \overline{Q_{obs}})^2} \sqrt{\sum_{i=1}^n (Q_{sim} - \overline{Q_{sim}})^2}} \right]^2$$

$$(14) \dots R^2 = \frac{\sum_{i=1}^n (Q_{obs} - \overline{Q_{obs}})(Q_{sim} - \overline{Q_{sim}})^2}{\sum_{i=1}^n (Q_{obs} - \overline{Q_{obs}})^2 (Q_{sim} - \overline{Q_{sim}})^2}$$

$$(15) \dots PBIAS = \frac{\sum_{i=1}^n (Q_{sim} - Q_{obs})}{\sum_{i=1}^n Q_{obs}} \times 100\%$$

$$(16) \dots NSE = 1 - \frac{\sum_{i=1}^n (Q_{obs} - Q_{sim})^2}{\sum_{i=1}^n (Q_{obs} - \overline{Q_{sim}})^2}$$

Prior to calibration and validation, a sensitivity analysis for the RRI model was performed in Wadi Mekerra to assess the relative importance of each model parameter in influencing the output hydrograph peak and shape.

The sensitivity analysis was conducted utilising the one-factor-at-a-time method, wherein just one parameter was altered during each simulation while the remaining parameters were held at their normal settings.

The configuration of significant sensitive RRI model parameters is presented in Table 4.1 The region's land use is defined by an arid mountainous area in the south and sparse vegetation along with urban development in the north, thus primarily influenced by surface runoff and infiltration (cases a and b). Case c is omitted from our analysis due to a drought that affected the study area during the summer prior to the autumn rainfall. The subsequent figure 4.10 is an illustration of RRI cases.

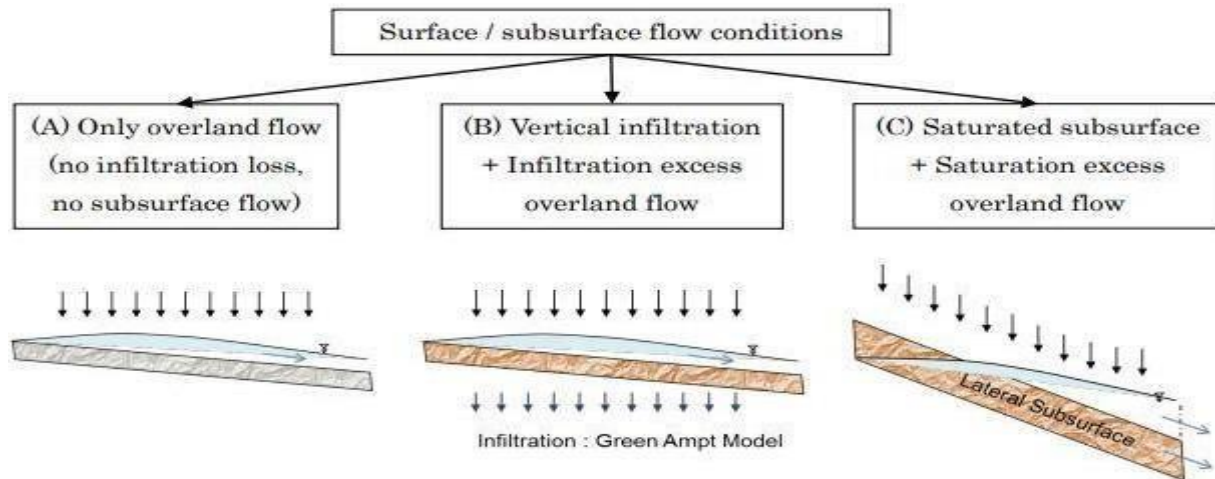


Fig 4.10: RRI cases

**Table 4.1:** RRI cases and limits of operation of these parameters.

Parameters	Units	Notation	Range	Cases <sup>1</sup>
Channel roughness coefficient	m-1/3s	ns_river	0.015 0.04	- a,b,c
Hillslope roughness coefficient	m-1/3s	ns_slope	0.15 - 1.0	a,b,c
Soil depth	m	soilepth	0.1 - 2.0	b,c
Soil porosity	-	gammaa	0.05 - 0.6	b,c
Vertical saturated hydraulic conductivity	ms <sup>-1</sup>	Kv	6.54×10 <sup>-5</sup> 1.67×10 <sup>-7</sup>	b,c
Suction at the vertical wetting front	m	Sf	0.0495 0.3163	- b,c
Lateral saturated hydraulic conductivity	ms <sup>-1</sup>	Ka	0.01 - 0.3	c
Unsaturation effective porosity	-	Gamma	0.02 - 0.4	c

The intensity of the flood can be assessed using the flood map produced by the RRI. The water depth at each location in the basin may be ascertained during the occurrence, facilitating comprehension of the flood pattern.

#### **4.4 Limitations of the methodology:**

Assessing the authenticity of the data and its scarcity is regarded as a significant difficulty that adversely impacts the methodological boundaries, particularly when selecting a flood occurrence from the past decade, thereby enhancing the research's credibility. Upon analyzing land use, it is observed that the disparity between the LULC during the year of the floods and the current LULC is not significant enough to influence the flood's trajectory or intensity.

#### **4.5 Conclusion**

This chapter has provided a detailed methodological framework for evaluating flood risk in the Mekerra Basin utilizing the Rainfall-Runoff-Inundation (RRI) model. The adopted methodology combines sophisticated hydrological modeling techniques with diverse geographical data to tackle the specific issues of flood simulation in semi-arid regions. Significant methodological contributions encompass the establishment of a rigorous calibration and validation methodology utilizing limited hydrological data, novel techniques for parameter estimation under data-constrained circumstances, and the incorporation of climate scenarios for forecasting future flood risk. The methodology's efficacy resides in its capacity to integrate physically-based process depiction with pragmatic solutions for the data limitations inherent to the studied area. The structured process from data preparation to model implementation and risk mapping offers a reproducible framework for flood evaluation in analogous semi-arid basins. The methodology, while recognizing inherent limitations in model parameterization and input data, presents a scientifically rigorous basis for the following examination of flood hazards and vulnerabilities in the Mekerra Basin. This modeling technique will enhance comprehension of flood dynamics in Algeria's semi-arid regions and offer practical insights for flood risk management and mitigation planning. Future enhancements may investigate higher-resolution climate data and integrated human-natural system interactions to improve the model's forecast accuracy.

# *Chapter 5:*

# Results and Discussion

## **5.1 Introduction:**

The principal objective of this research was to evaluate flood risk in the Mekerra basin utilizing the Rainfall-Runoff-Inundation (RRI) model, aiming to improve flood forecasting and guide disaster risk management techniques. This chapter delineates the outcomes of employing the RRI model for flood risk assessment, emphasizing the precision of the model simulations. The findings are categorized into three primary sections: Sensitivity Analysis, Calibration and Validation Results, and Simulation of the Mekerra Flash Flood Event. This analysis examines the effects of differing rainfall intensities, alterations in land use, and hydrological parameters on flood risk patterns. The results elucidated herein enhance comprehension of flood dynamics in the region, with possible ramifications for flood preparedness, policy formulation, and further modeling initiatives.

## **5.2 Sensitivity Analysis:**

This study analyzed the responsiveness of the RRI model to critical hydrological parameters, such as hydraulic conductivity ( $k_{sv}$ ), Manning's roughness coefficient ( $n_{river}$ ), and suction head ( $S_f$ ). Each parameter substantially affects the timing, magnitude, and duration of flood peaks, underscoring the necessity of precise parameter calibration in flood modeling.

In Figure 5.1, the variable altered was hydraulic conductivity ( $k_{sv}$ ), which denotes a material's capacity to convey water and is crucial for comprehending groundwater flow and transport in aquifers. Reduced hydraulic conductivity results in diminished water infiltration into the soil, leading to increased and concentrated runoff (Ralwls, 1992) . A hydraulic conductivity of  $k_{sv} = 1.67 \times 10^{-7}$  demonstrated a pronounced peak discharge of roughly  $500 \text{ m}^3/\text{s}$ , occurring at around 20 hours. Conversely, elevated  $k_{sv}$  values (e.g.,  $6.54 \times 10^{-5}$ ) and the standard  $k_{sv}$  curve, indicative of the original uncalibrated parameter utilized in the model, exhibited diminished peak discharges of around 120 and  $100 \text{ m}^3/\text{s}$ , respectively. The diminished peaks indicate an enhanced infiltration capability, resulting in more water absorption by the soil and a reduction in surface runoff intensity.

Numerous research have employed the RRI model to comprehend and forecast flood occurrences, doing comprehensive sensitivity analysis to ascertain critical factors. A research in Wadi Samail,

Oman, revealed the channel roughness coefficient ( $n_{\text{river}}$ ) and hillslope roughness coefficient ( $n_{\text{slope}}$ ) as the most relevant characteristics, followed by soil depth ( $d$ ) and soil porosity ( $\phi$ ) (Abdel-Fattah et al., 2018).

Our sensitivity analysis similarly underscored the significance of hydraulic conductivity ( $k_{\text{sv}}$ ), Manning's roughness coefficient ( $n_{\text{river}}$ ), and suction head ( $S_f$ ), which were essential for precisely modeling the flash flood episodes in Mekerra. A study in Yangon City, Myanmar, employed the RRI model to simulate flood events, with sensitivity analysis concentrating on lateral saturated hydraulic conductivity ( $k_a$ ) and soil depth ( $h_d$ ) (San et al., 2020). The findings indicated substantial variations in these parameters attributable to the geological features and climatic zones of Myanmar.

Figure 5.3 illustrates the fluctuation of Manning's roughness coefficient ( $n_{\text{river}}$ ) for river flow in Mekerra. Manning's  $n$  is a crucial measure for assessing flow resistance; reduced roughness leads to accelerated water movement and more concentrated flood peaks (Mohanta et al., 2018). A river value of 0.015, indicative of a lower roughness coefficient, exhibited the most pronounced peak flow of approximately 200  $\text{m}^3/\text{s}$ , whereas a higher roughness coefficient demonstrated increased flow resistance, leading to energy losses. Manning's coefficient ( $n$ ) is essential for calculating flood discharge and velocity dispersion (Azamathulla et al., 2012).

Figure 5.2 examines the influence of the suction head ( $S_f$ ) parameter on the resultant hydrograph.  $S_f$  is a metric related to the infiltration qualities of soil. It quantifies the pressure differential in the soil due to its moisture content, reflecting the soil's capacity to withstand gravitational forces and retain water (Sun et al., 2023). During floods, suction head is essential in influencing the rate and effectiveness of water infiltration into the soil. An elevated suction head typically signifies more water retention by the soil. A reduced suction head may lead to heightened surface runoff. The data indicates that at  $s_f = 0.0495$ , indicative of a smaller suction head, the peak discharge reached roughly 500  $\text{m}^3/\text{s}$ , whereas at  $s_f = 0.3163$ , the peak discharge significantly decreased to around 100  $\text{m}^3/\text{s}$ .

The sensitivity analysis results indicate that the simulated hydrographs underestimated the measured flow due to the use of a single-variable testing method, in which only one parameter was modified during each simulation while all other parameters remained at their default values.

While parameters like vertical saturated hydraulic conductivity, suction at the vertical wetting front, and channel roughness coefficient displayed considerable fluctuations in the hydrograph between their maximum and minimum values, other parameters, such as hillslope roughness coefficient, soil depth, and soil porosity, did not significantly influence the hydrograph.

The findings indicate that changes in these factors substantially affect flood peak timing, amplitude, and duration, offering important insights into the fundamental hydrological processes. Reduced  $k_{sv}$  values led to swift runoff and pronounced flood peaks, indicative of the characteristics of impermeable soils like clay. In contrast, elevated  $k_{sv}$  values improved infiltration, diminishing flood severity and postponing peak discharge, highlighting the significance of soil permeability control.

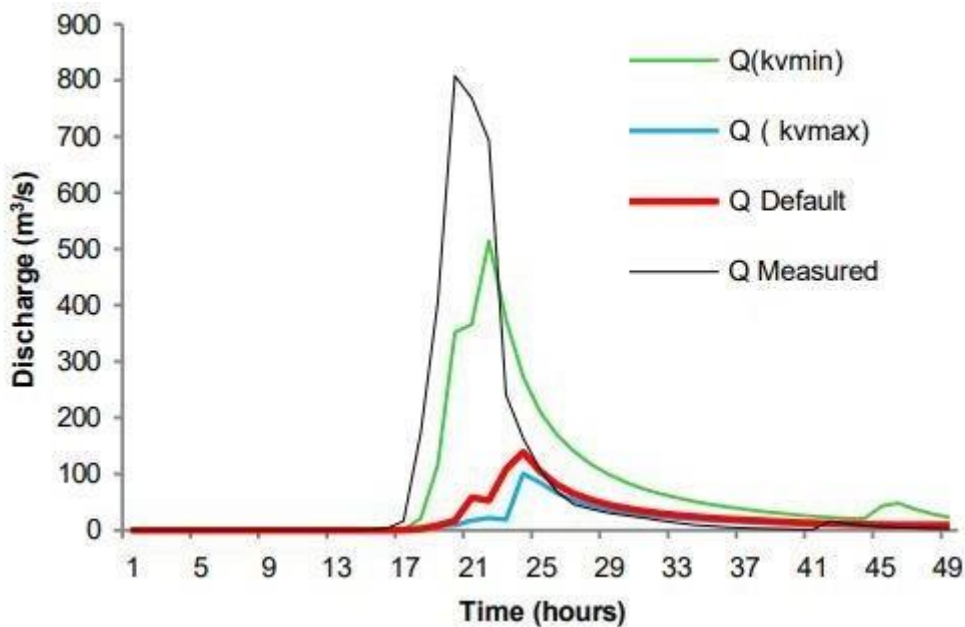


Fig 5.1 : Simulated hydrograph variations of vertical saturated hydraulic conductivity ( $K_{sv}$ ), showing how a higher  $K_v$  value reduces flood peaks through enhanced infiltration

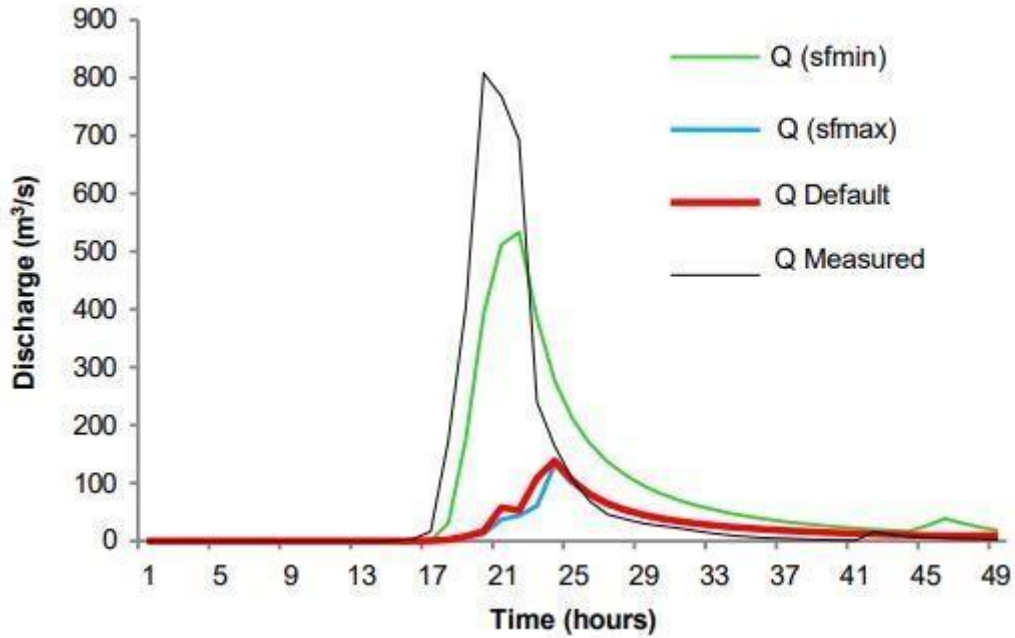


Fig 5.2: Simulated hydrograph variations of suction at the vertical wetting front (Sf), illustrating the impact of soil water retention on surface runoff

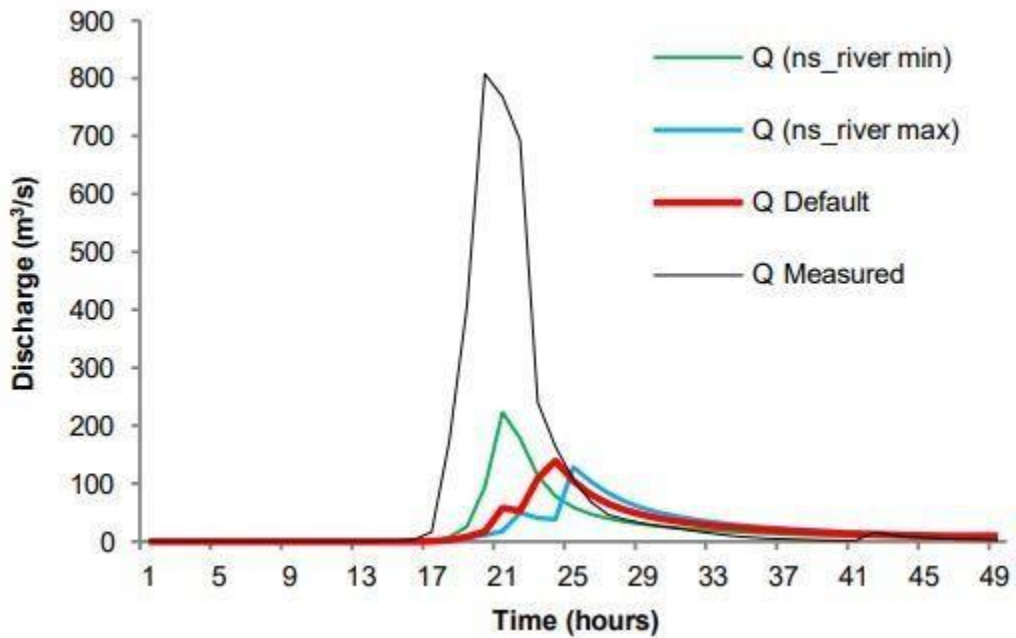


Fig 5.3: Simulated hydrograph variations channel roughness coefficient (ns\_river), emphasizing the role of flow resistance in moderating flood peaks.

### 5.3 Calibration and Validation Results

The RRI model shown commendable efficacy in modeling flash flood occurrences in the Mekerra Basin, as indicated by its calibration and validation metrics in Table 5.1. The elevated correlation coefficients (0.97 for the 1986 incident and 0.94 for the 1994 event) signify a robust concordance between the observed and simulated data. The Nash–Sutcliffe Efficiency (NSE) ratings of 0.93 and 0.86 for the calibration and validation events, respectively, indicate the model's proficiency in capturing the timing and amplitude of peak discharges. The findings align with earlier research in the Mekerra Basin utilizing the MERCEDES model, which established NSE values over 0.80 as a standard for satisfactory model performance (Maref & Seddini, 2018b) . A research utilizing the Runge–Kutta Discontinuous Galerkin (RKDG) finite element method to simulate historical floods in Wadi Mekerra demonstrated great accuracy, with a discharge discrepancy of merely 1.17% during the 1983 flood event (Atallah et al., 2016b).

Furthermore, (Korichi et al., 2016b) utilized two hydraulic modeling approaches, the Van Leer Finite Volume method and the Petrov–Galerkin method, to replicate the flood occurrences of 1983 and 1995 in Wadi Mekerra. In the 1983 event, the Van Leer approach attained a relative error of 4.96%, but the Petrov–Galerkin method produced an error of 14.65%. In the 1995 event, the relative errors were 0.24% for the Van Leer approach and 1.64% for the Petrov–Galerkin method.

Nevertheless, despite the favorable outcomes achieved with the RRI model in this study, there remain opportunities for enhancement. The model overestimated flood levels by 8.2% during the 1986 calibration event and underestimated them by 24.3% during the 1994 validation event. These variations indicate that although the model well represents basic flood behavior, it may falter in providing accurate volumetric predictions for various occasions.

**Table 5.1:** RRI parameter value of calibration

				Calibration		
Parameter	Unit	Notation				
			Crops	Land Use	Built Area	
Channel roughness coefficient	$m^{-1}/3_s$	ns_river	0.015	0.015	0.015	
Hillslope roughness coefficient	$m^{-1}/3_s$	ns_slope	0.15	0.15	0.15	
Soil depth	M	soilepth	0.45	1	2.0	
Soil porosity	-	gamma_a	0.3	0.1	0.05	
Vertical saturated hydraulic conductivity	$ms^{-1}$	Kv	$1.67 \times 10^{-7}$	$1.45 \times 10^{-6}$	x	
Suction at the vertical wetting front	M	Sf	0.2185	0.2045	x	
Lateral saturated hydraulic conductivity	$m.s^{-1}$	Ka	x	X	x	
Unsaturation effective porosity	-	Gamma_a	x	X	x	

**Table 5.2:** RRI model performance metrics for calibration and validation.

<b>Performance Characteristic</b>	<b>Calibration (1986 Event)</b>	<b>Validation (1994 Event)</b>
Correlation Coefficient	0.97	0.94
$r^2$	0.94	0.89
PBIAS	0.006	0.013
NSE	0.93	0.86

## **5.4 Simulation of Mekerra Flash Flood Event**

Floods have inflicted significant devastation during the last forty years. The most catastrophic flood transpired on 04 October 1986 in Sidi Bel Abbes (, with a discharge rate of 800 m<sup>3</sup>/s, resulting in three fatalities, nearly 1000 residents rendered homeless, and impacting 530 persons and 200 households.

Appendix A1 displays a simulation of runoff dynamics associated with the 1994 flood event, generated using the Rainfall–Runoff–Inundation (RRI) model interface. The system enables users to determine flow rates and water depths at any spatial location within the basin by selecting the desired point directly on the program interface, thus providing flexible access to hydrodynamic information for model validation and analysis. Appendix A2 specifically represents the output obtained by selecting the location of the Sidi Ali Ben Youb hydrometric station within the interface during the 1994 event, allowing direct visualization of simulated discharge and water level time series at this monitoring point. This functionality underscores the model’s capacity for site-specific hydrological assessment and supports detailed validation against observed data.

Figures 5.4 and 5.5 present hydrographs that represent the hydrological events of October 1986 and September 1994. These events signify the most severe catastrophic disasters, marked by considerable loss of life and extensive economic destruction within the watershed.

Both events are classified as flash floods. The 1986 event focused on calibrating the RRI model, whereas the 1994 event aimed to validate it. In both instances, the increase in water levels was swift, occurring in under 4 hours, shifting from an extremely insignificant base flow to a peak

flow of 808 m<sup>3</sup>/s for the calibration event and 236 m<sup>3</sup>/s for the validation event. Both incidents demonstrated significant increases, with an extraordinary rise of over 400 m<sup>3</sup>/s per hour for the first event and around 188 m<sup>3</sup>/s for the second.

The calibration model simulated flood persisted for merely 21 hours, from around 10 to 20 hours. The floodwater intake was  $13.46 \times 10^6$  m<sup>3</sup> (observed) versus  $14.57 \times 10^6$  m<sup>3</sup> simulated by the RRI model, leading to an overestimation of 8.2% relative to the observed flood. The flood's rising flow persisted for under 4 hours, with an observed volume input of approximately 37%, in contrast to the simulated figure of 30%. In assessing water quantities throughout a dynamic 3-hour time frame, the important input was that pertaining to the period 1 hour prior to the peak and 1 hour subsequent to it. This window indicates a significant risk of river overflow. In the crucial calibration flood period, the water input constituted 53.0% of the total input based on observed values and 46.4% based on simulated values, resulting in an error of merely -5.4%.

The validation flood persisted for 37 hours, with an estimated water discharge volume of  $5.23 \times 10^6$  m<sup>3</sup> in the observed data and  $3.96 \times 10^6$  m<sup>3</sup> in the simulated data, leading to an underestimation of roughly -24.3%. The water volume contribution during the critical window was around 42.6% in the actual data and 51.8% in the simulated data. The error margin was merely -8.0%.

The distinctions in the attributes of the 1986 and 1994 flood episodes may elucidate the noted inconsistencies in the volumetric estimations. The 1986 flood, characterized by a shorter duration and greater intensity, seemed to correspond more accurately with the model's calibration parameters. The swift increase in water levels and elevated peak discharge certainly aligned with the characteristics optimal for severe flash floods. In contrast, the extended length of the 1994 flood, marked by a gradual rise in flow rates and diminished peak discharge, likely required modifications to accommodate ongoing infiltration, subsurface contributions, and extended runoff processes. The fluctuations in peak discharge and flood duration indicate that event-specific characteristics substantially affect model performance, highlighting the necessity to adjust parameters for improved flexibility across various hydrological circumstances.

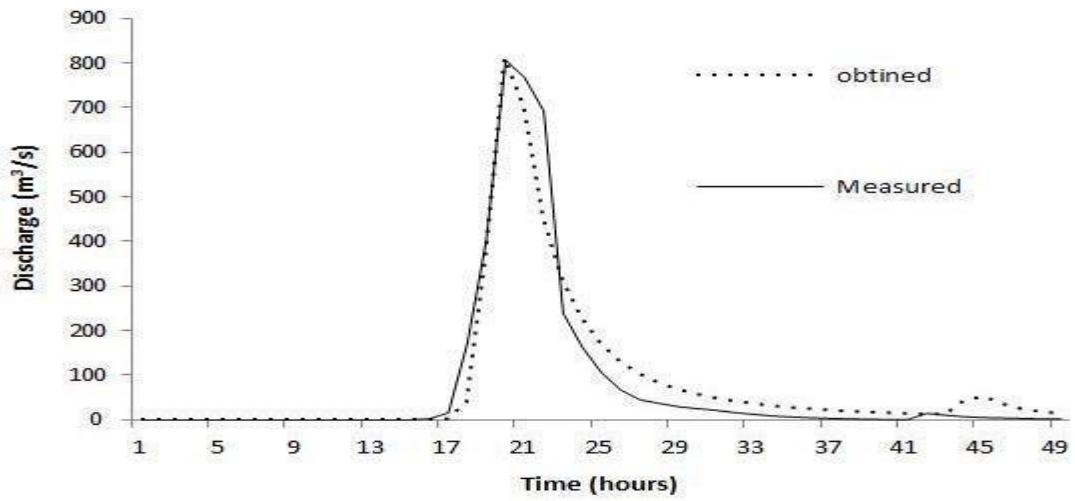


Fig 5.4 : Simulation of Mekerra flash flood event RRI model calibration results for 1986 event

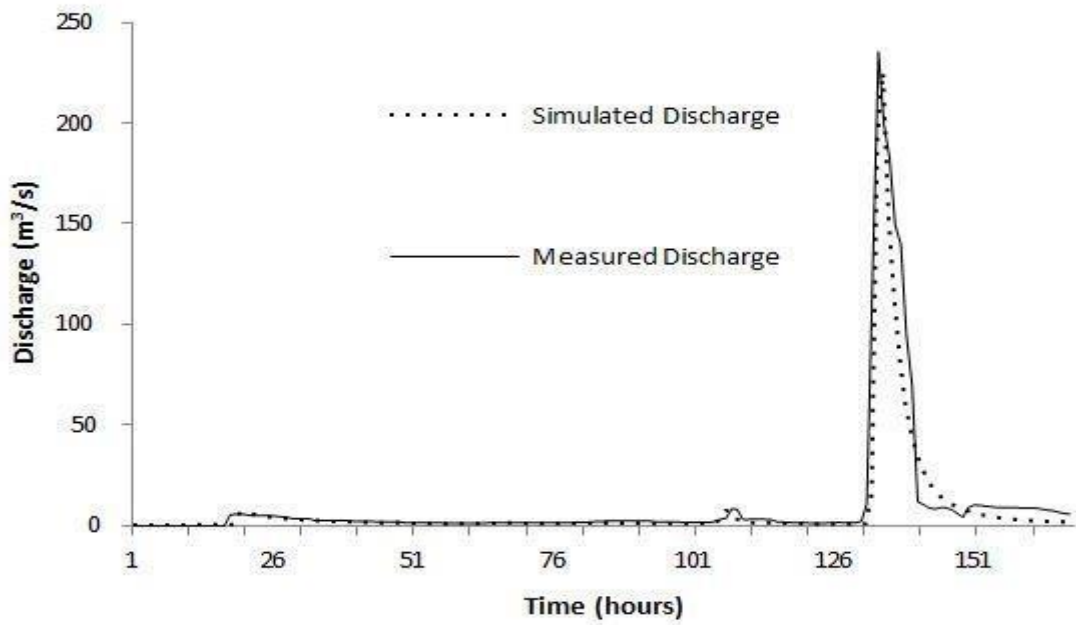


Fig 5.5: Simulation of Mekerra flash flood event RRI model validation results for 1994 event

## 5.5 Comparison with other models used Mekerra basin

The comparative evaluation of modeling results draws upon two prior studies conducted by Maref (2018) and Atallah (2017), which together provide a comprehensive examination of flood risk within the Wadi Mekerra basin in northwestern Algeria. The first study addresses hydrological processes at the catchment scale, employing the MERCEDES distributed hydrological model to simulate rainfall–runoff transformation across a semi-arid basin. Despite achieving satisfactory overall performance, the model exhibits systematic underestimation of peak flows, primarily attributed to localized convective precipitation and sensitivity to seasonal variations in land cover. Complementarily, the second study adopts a high-resolution two-dimensional hydrodynamic modeling approach for the urban center of Sidi Bel Abbes, focusing on a 5.4 km river segment to simulate floodplain inundation dynamics under extreme hydrological scenarios. Its primary objective lies in the generation of detailed flood hazard maps to support urban defense and risk management planning. Taken together, these studies establish a coherent methodological progression from basin-scale runoff quantification to localized floodplain inundation assessment. This two-tiered modeling framework, which effectively decouples watershed hydrology from channel hydraulics, offers a robust foundation for comparison with the integrated Rainfall–Runoff–Inundation (RRI) model.

A critical comparative analysis of the MERCEDES, Runge–Kutta, and RRI models underscores substantive differences in their validation protocols, physical parameterization, and overall predictive performance. The MERCEDES model demonstrates substantial robustness through multi-event calibration (2003–2012), whereas both the Runge–Kutta and RRI models were verified against a single event an approach that, though limiting, permits controlled inter-model comparison. In this context, the RRI model exhibits superior correspondence between simulated and observed hydrographs, particularly in reproducing the timing and magnitude of peak discharge (figure 5.6) . This superiority arises from its conceptual framework, which explicitly incorporates key soil parameters such as porosity and permeability. By contrast, the Runge–Kutta formulation omits these factors, reducing its physical fidelity in representing infiltration-driven runoff generation. Both the MERCEDES and RRI models demonstrate high Nash–Sutcliffe efficiency ( $NSE \geq 0.8$ ); however, the RRI model’s distinctive merit lies in its integrative coupling

of rainfall–runoff and inundation processes throughout the Mekerra Basin. This unified structure enables extraction of water depth and velocity data at any spatial location, yielding a comprehensive platform for basin-wide flood forecasting that surpasses the more compartmentalized designs of the other two models.

Notwithstanding their contributions, both earlier studies display notable methodological limitations. The MERCEDES based analysis systematically underestimates peak flows by as much as 60 percent, significantly constraining its predictive validity for flood forecasting and infrastructure design. Although the authors attribute this discrepancy primarily to rainfall input uncertainties, potential structural deficiencies in the MERCEDES model’s representation of semi-arid convective hydrology appear unexamined. Moreover, the recommendation of large-scale reforestation as a flood mitigation strategy, while conceptually reasonable, is advanced without a quantitative assessment of scope or species typology, leading to an overly speculative conclusion. Similarly, the hydrodynamic modeling of Atallah (2017), despite its technical sophistication, yields conclusions of limited originality principally emphasizing expected relationships between topography, flow velocity, and inundation extent.

In aggregate, the MERCEDES and Runge–Kutta frameworks remain valuable for addressing specific hydrological or hydraulic research objectives in the Mekerra basin. Nevertheless, the RRI model emerges as a more comprehensive and operationally coherent tool. Its capacity to unify runoff generation and inundation processes within a single spatially continuous environment provides an enhanced basis for integrated basin management. By enabling end-to-end simulation of the flood sequence from rainfall initiation to overland flow propagation the RRI model establishes itself as a powerful analytical instrument for flood risk assessment, offering both scientific rigor and practical applicability for regional water resource planning.

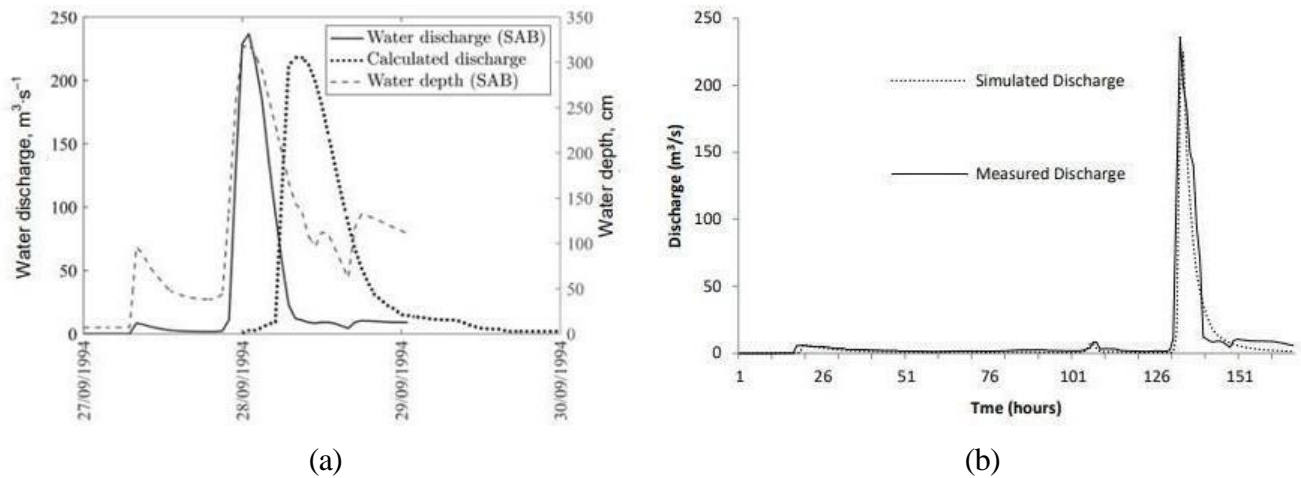


Figure 5.6 : Simulation of September 1994 flood event : (a) Runge–Kutta model simulation results; (b) RRI model simulation results Runge–Kutta model simulation results.

## 5.6 Conclusion:

This study is the inaugural application of the Rainfall–Runoff–Inundation (RRI) model in the Mekerra Basin, a flood-prone region in northern Algeria. This research, through meticulous calibration and validation with data from major flood occurrences in 1986 and 1994, established the RRI model's efficacy in reproducing flood dynamics in semi-arid environments, attaining correlation coefficients of 0.97 and 0.94 for the relevant events. The sensitivity studies indicated three pivotal characteristics affecting flood peaks: hydraulic conductivity, suction head, and channel roughness. Reduced hydraulic conductivity values ( $1.67 \times 10^{-7}$ ) yielded pronounced peak discharges of roughly  $500 \text{ m}^3/\text{s}$ , whereas elevated values ( $6.54 \times 10^{-5}$ ) led to diminished peaks near  $120 \text{ m}^3/\text{s}$ , illustrating the substantial influence of this parameter on runoff dynamics. Manning's roughness coefficient exhibited significant impact, with diminished values (0.015) resulting in more pronounced peaks at  $200 \text{ m}^3/\text{s}$ .

The model exhibited robust performance measures, achieving Nash–Sutcliffe Efficiency (NSE) values of 0.93 during calibration and 0.86 during validation, alongside  $R^2$  values of 0.94 and 0.89, respectively. Significant disparities were noted in the volumetric predictions: the model overestimated the 1986 flood volume by 8.2% ( $14.57 \times 10^6 \text{ m}^3$  (simulated) vs.  $13.4 \times 10^6 \text{ m}^3$  (observed)) and underestimated the 1994 flood volume by 24.3% ( $3.96 \times 10^6 \text{ m}^3$  (simulated) vs.  $5.2 \times 10^6 \text{ m}^3$  (observed)).

(simulated) vs  $5.23 \times 10^6 \text{ m}^3$  (observed).

The model exhibited considerable variations in performance attributable to the unique characteristics of the flood episodes. The 1986 flood included a brief period of 21 hours and a peak flow of  $808 \text{ m}^3/\text{s}$ , whereas the 1994 event had an extended duration of 37 hours with a reduced peak discharge of  $236 \text{ m}^3/\text{s}$ . The inherent disparities in flood behavior impeded the model's capacity to accurately replicate both occurrences using a singular parameter combination.

The study encountered certain constraints that must be acknowledged when analyzing the findings. Constraints in data availability, specifically the dependence on merely two previous flood events for calibration and validation, adversely affected the model's robustness. The limits in temporal resolution of rainfall data hindered the model's capacity to detect quick flood start. The region's semi-arid characteristics and the scarcity of ground-truth data created ambiguity in parameter estimation.

Future research endeavors should concentrate on augmenting the model's capabilities via many critical enhancements. Although satellite-derived rainfall data can assist in filling precipitation data gaps, it is crucial to possess observed flood event data for model refinement.

*Chapter 6:*  
Conclusions

## 6.1 CONCLUSION:

This PhD thesis presents a comprehensive flood risk assessment of Algeria's Mekerra Basin through the development and application of an advanced Rainfall-Runoff-Inundation (RRI) modeling framework, representing a significant contribution to both hydrological science and practical flood management in semi-arid regions. The research effectively tackled the significant issues of modeling flash flood dynamics in data-deficient settings by creating novel methods for parameter estimate, data integration, and uncertainty quantification. The RRI model shown robust prediction capacity (NSE=0.86, R<sup>2</sup>=0.89) through meticulous calibration and validation against historical flood occurrences, especially in replicating the swift hydrological responses typical of the basin's steep topography and heavy rainfall patterns. These findings have significant implications for regional water resource management and disaster preparedness, offering the inaugural precise, scientifically-based flood hazard maps for the Mekerra Basin that explicitly consider present vulnerabilities . The study's methodological advancements, such as the amalgamation of multi-source satellite data with sparse ground observations and the creation of a replicable framework for uncertainty analysis, provide significant models for flood risk assessment in analogous data-deficient areas throughout North Africa and the Mediterranean. This research provides practical tools for decision-makers, such as prioritized lists of high-risk neighborhoods, recommendations for infrastructure enhancements, and guidelines for land-use planning rules, in addition to its scientific contributions. This study enhances our comprehension of semi-arid flood dynamics while pinpointing significant knowledge deficiencies that require additional research, especially concerning the interactions between surface water and groundwater systems during extreme events, the effects of evolving land-use patterns on flood risk, and the advancement of more effective climate downscaling methodologies for the region. By bridging the gap between theoretical hydrology and applied risk reduction strategies, this thesis establishes a foundation for evidence-based flood management in the Mekerra Basin while contributing transferable methodologies that can enhance resilience to increasing flood risks under climate change throughout semi-arid watersheds globally. The results highlight the immediate necessity for adaptive management strategies that combine scientific expertise with local stakeholder involvement to create effective, sustainable solutions for one of Algeria's most critical environmental issues.

## 6.2 Recommendations

This PhD study concludes with a set of strategic recommendations that tackle immediate requirements and foster long-term resilience development. The findings highlight the critical need for improved hydrological monitoring via an expanded network of automated weather stations, stream gauges, and the incorporation of advanced remote sensing technologies such as Sentinel-1 SAR data for flood extent mapping, along with UAV-based topographic surveys to enhance model precision. The study emphatically supports the creation of a comprehensive flood forecasting system that integrates RRI model outputs with machine learning algorithms to improve prediction accuracy, especially for flash flood occurrences that define the basin's hydrology. The study advocates for prioritized investments in nature-based solutions, such as upstream retention ponds and restored floodplains, in conjunction with engineered interventions like enhanced stormwater drainage systems in high-risk urban areas, including Hacaiba, Sidi Ali Benyoub, and Sidi Belabbas, with design standards informed by the 100-year flood projections from this study. Policy proposals advocate for the formal incorporation of the developed flood hazard maps into Algeria's National Adaptation Plan, alongside targeted revisions to land-use zoning restrictions that restrict key infrastructure development in high-risk areas identified by the modeling. The report advocates for a multi-faceted awareness initiative at the community level, incorporating local flood preparedness training, multilingual risk communication resources, and the creation of community-based early warning systems connected to the national meteorological service. The recommendations underscore the necessity of enhancing institutional capacity via specialized training programs in flood modeling for Algerian water authorities, alongside the establishment of a regional research consortium to improve flood risk assessment methodologies in North African semi-arid basins. The study finds significant knowledge gaps that necessitate more exploration, including the effects of altered agricultural practices on runoff generation and the possibility for groundwater recharge during flood events as a method for climate adaptation. These detailed recommendations, based on the study's rigorous modeling framework and risk assessment, offer a practical guide for converting the Mekerra Basin from a flood-prone to a flood-resilient system, while providing applicable insights for analogous semi-arid regions worldwide confronting heightened flood risks due to climate change.

## References

- Abbes, A. S. B., & Meddi, M. (2016). Study of propagation and floods routing in north-western region of Algeria. *International Journal of Hydrology Science and Technology*, 6(2), 118. <https://doi.org/10.1504/ijhst.2016.075578>
- Abdel-Fattah, M., Kantoush, S. A., Saber, M., & Sumi, T. (2018). RAINFALL-RUNOFF MODELING FOR EXTREME FLASH FLOODS IN WADI SAMAIL, OMAN. *Journal of Japan Society of Civil Engineers Ser B1 (Hydraulic Engineering)*, 74(5), I\_691-I\_696. [https://doi.org/10.2208/jscejhe.74.5\\_i\\_691](https://doi.org/10.2208/jscejhe.74.5_i_691)
- Abdelgawad, A. G., Helal, E., Sobeih, M. F., & Elsayed, H. (2024). Flood hazard mapping using a GIS-based morphometric analysis approach in arid regions, a case study in the Red Sea Region, Egypt. *Applied Water Science*, 14(4). <https://doi.org/10.1007/s13201-024-02130-5>
- Abdeta, G. C., Tesemma, A. B., Tura, A. L., & Atlabachew, G. H. (2020). Morphometric analysis for prioritizing sub-watersheds and management planning and practices in Gidabo Basin, Southern Rift Valley of Ethiopia. *Applied Water Science*, 10(7). <https://doi.org/10.1007/s13201-020-01239-7>
- Abrar, M. F., Iman, Y. E., Mustak, M. B., & Pal, S. K. (2024). Assessment of vulnerability to flood risk in the Padma River Basin using hydro-morphometric modeling and flood susceptibility mapping. *Environmental Monitoring and Assessment*, 196(7). <https://doi.org/10.1007/s10661-024-12780-2>
- Adhikari, S. (2020). Morphometric analysis of a drainage basin: A study of Ghatganga River, Bajhang District, Nepal. *The Geographic Base*, 7, 127–144. <https://doi.org/10.3126/tgb.v7i0.34280>

- Alarifi, S. S., Abdelkareem, M., Abdalla, F., & Alotaibi, M. (2022). Flash flood hazard mapping using remote sensing and GIS techniques in southwestern Saudi Arabia. *Sustainability*, *14*(21), 14145. <https://doi.org/10.3390/su142114145>
- Al-Delaimy, W. K. (2020). Vulnerable Populations and Regions: Middle East as a case study. In *Springer eBooks* (pp. 121–133). [https://doi.org/10.1007/978-3-030-31125-4\\_10](https://doi.org/10.1007/978-3-030-31125-4_10)
- Aloui, S., Mazzoni, A., Elomri, A., Aouissi, J., Boufekane, A., & Zghibi, A. (2022). A review of Soil and Water Assessment Tool (SWAT) studies of Mediterranean catchments: Applications, feasibility, and future directions. *Journal of Environmental Management*, *326*, 116799. <https://doi.org/10.1016/j.jenvman.2022.116799>
- Arnaud-Fassetta, G., Astrade, L., Bardou, É., Corbonnois, J., Delahaye, D., Fort, M., Gautier, E., Jacob, N., Peiry, J., Piégay, H., & Penven, M. (2009). Fluvial geomorphology and flood-risk management. *Géomorphologie Relief Processus Environnement*, *15*(2), 109–128. <https://doi.org/10.4000/geomorphologie.7554>
- Atallah, M., Djellouli, F., & Hazzeb, A. (2024, March 22). *RAINFALL-RUNOFF MODELING USING THE HEC-HMS MODEL FOR THE MEKERRA WADI WATERSHED (N-W ALGERIA)*. ATALLAH | LARHYSS Journal P-ISSN 1112-3680 / E-ISSN 2521-9782. <http://larhyss.net/ojs/index.php/larhyss/article/view/13824>
- Atallah, M., Hazzab, A., Seddini, A., Ghenaim, A., & Korichi, K. (2016a). Hydraulic flood routing in an ephemeral channel: Wadi Mekerra, Algeria. *Modeling Earth Systems and Environment*, *2*(4), 1–12. <https://doi.org/10.1007/s40808-016-0237-0>
- Atallah, M., Hazzab, A., Seddini, A., Ghenaim, A., & Korichi, K. (2016b). Hydraulic flood routing in an ephemeral channel: Wadi Mekerra, Algeria. *Modeling Earth Systems and Environment*, *2*(4), 1–12. <https://doi.org/10.1007/s40808-016-0237-0>
- Awawdeh, M., Mhedat, M., & Alkhatib, S. (2024). Morphometric analysis and prioritization of watersheds for flash floods management in Wadi Arab Catchment, North Jordan.

*Dirasat Human and Social Sciences*, 51(5), 249–262.

<https://doi.org/10.35516/hum.v51i5.4135>

Azamathulla, H. M., Ahmad, Z., & Ghani, A. A. (2012). An expert system for predicting Manning's roughness coefficient in open channels by using gene expression programming. *Neural Computing and Applications*, 23(5), 1343–1349.

<https://doi.org/10.1007/s00521-012-1078-z>

Ballesteros, C., Jiménez, J. A., & Viavattene, C. (2017). A multi-component flood risk assessment in the Maresme coast (NW Mediterranean). *Natural Hazards*, 90(1), 265–292. <https://doi.org/10.1007/s11069-017-3042-9>

Barrocu, G., & Eslamian, S. (2022). Geomorphology and flooding. In *CRC Press eBooks* (pp. 23–54). <https://doi.org/10.1201/9781003262640-3>

Bashir, B., & Alsalman, A. (2024). Morphometric characterization and dual analysis for flash flood hazard assessment of Wadi Al-Lith Watershed, Saudi Arabia. *Water*, 16(22), 3333. <https://doi.org/10.3390/w16223333>

Boutaghane, H., Boulmaiz, T., Lameche, E. K., Lefkir, A., Hasbaia, M., Abdelbaki, C., Moulahoum, A. W., Keblouti, M., & Bermad, A. (2021). Flood analysis and mitigation strategies in Algeria. In *Natural disaster science and mitigation engineering: DPRI reports* (pp. 95–118). [https://doi.org/10.1007/978-981-16-2904-4\\_3](https://doi.org/10.1007/978-981-16-2904-4_3)

Brunner, M. I., Slater, L., Tallaksen, L. M., & Clark, M. (2021). Challenges in modeling and predicting floods and droughts: A review. *Wiley Interdisciplinary Reviews Water*, 8(3). <https://doi.org/10.1002/wat2.1520>

Chen, X., Liang, B., Li, J., Cai, Y., & Liang, Q. (2024). Comprehensive Assessment of Large-Scale Regional Fluvial Flood Exposure Using Public Datasets: A Case Study

- from China. *ISPRS International Journal of Geo-Information*, 13(10), 357.  
<https://doi.org/10.3390/ijgi13100357>
- CONVENTION DES NATIONS UNIES SUR LE DROIT DE LA MER. (1998). *Journal Officiel Des Communauté S Europe Ennes*.
- [Convention des Nations Unies sur le droit de la mer du 10 décembre 1982]. (1982). [Book].  
In *Convention des Nations Unies sur le droit de la mer*.
- Cunha, N., Magalhães, Domingos, T., Abreu, M., & Küpfer, C. (2017). The land morphology approach to flood risk mapping: An application to Portugal. *Journal of Environmental Management*, 193, 172–187. <https://doi.org/10.1016/j.jenvman.2017.01.077>
- Dwarakish, G. S., Pai, B. J., & Rajeesh, R. (2024). Urban flood hazard zonation in Bengaluru Urban District, India. *Journal of Landscape Ecology*, 17(1), 89–106.  
<https://doi.org/10.2478/jlecol-2024-0006>
- Elizabeth A, Hasenmueller and Robert E. Criss. (2013). Water Balance Estimates of Evapotranspiration Rates in Areas with Varying Land Use. In InTech eBooks.  
<https://doi.org/10.5772/52811>
- El-Nasr, A. A., Arnold, J. G., Feyen, J., & Berlamont, J. (2005). Modelling the hydrology of a catchment using a distributed and a semi-distributed model. *Hydrological Processes*, 19(3), 573–587. <https://doi.org/10.1002/hyp.5610>
- Farhan, Y., Anaba, O., & Salim, A. (2016). Morphometric analysis and flash floods assessment for drainage basins of the Ras en Naqb area, South Jordan using GIS. *Journal of Geoscience and Environment Protection*, 04(06), 9–33.  
<https://doi.org/10.4236/gep.2016.46002>
- Gajbhiye, S., Mishra, S. K., & Pandey, A. (2013a). Prioritizing erosion-prone area through morphometric analysis: an RS and GIS perspective. *Applied Water Science*, 4(1), 51–61. <https://doi.org/10.1007/s13201-013-0129-7>

Gajbhiye, S., Mishra, S. K., & Pandey, A. (2013b). Prioritizing erosion-prone area through morphometric analysis: an RS and GIS perspective. *Applied Water Science*, 4(1), 51–61. <https://doi.org/10.1007/s13201-013-0129-7>

- Ghenim, A. N., & Megnounif, A. (2016). Variability and trend of annual maximum daily rainfall in northern Algeria. *International Journal of Geophysics*, 2016, 1–11.  
<https://doi.org/10.1155/2016/6820397>
- Graf H., Altinakar M. S., 1996, *Hydraulique fluviale. Tome 2, Écoulement non permanent et phénomènes de transport*. Lausanne : Presses polytechniques et universitaires romandes.
- Hafnaoui, M., Boultif, M., & Dabanli, I. (2023a, December 26). *FLOODS IN ALGERIA: ANALYZES AND STATISTICS*. HAFNAOUI | LARHYSS Journal P-ISSN 1112-3680 / E-ISSN 2521-9782. <http://larhyss.net/ojs/index.php/larhyss/article/view/13788>
- Hafnaoui, M., Boultif, M., & Dabanli, I. (2023b, December 26). *FLOODS IN ALGERIA: ANALYZES AND STATISTICS*. HAFNAOUI | LARHYSS Journal P-ISSN 1112-3680 / E-ISSN 2521-9782. <http://larhyss.net/ojs/index.php/larhyss/article/view/13788>
- Hafnaoui, M., Boultif, M., & Dabanli, I. (2023c, December 26). *FLOODS IN ALGERIA: ANALYZES AND STATISTICS*. HAFNAOUI | LARHYSS Journal P-ISSN 1112-3680 / E-ISSN 2521-9782. <http://larhyss.net/ojs/index.php/larhyss/article/view/13788>
- Han, F., Yu, J., Zhou, G., Li, S., & Sun, T. (2024a). Projected urban flood risk assessment under climate change and urbanization based on an optimized multi-scale geographically weighted regression. *Sustainable Cities and Society*, 112, 105642.  
<https://doi.org/10.1016/j.scs.2024.105642>
- Han, F., Yu, J., Zhou, G., Li, S., & Sun, T. (2024b). Projected urban flood risk assessment under climate change and urbanization based on an optimized multi-scale geographically weighted regression. *Sustainable Cities and Society*, 112, 105642.  
<https://doi.org/10.1016/j.scs.2024.105642>
- Hill, B., Liang, Q., Boshier, L., Chen, H., & Nicholson, A. (2023). A systematic review of natural flood management modelling: Approaches, limitations, and potential

- solutions. *Journal of Flood Risk Management*, 16(3).  
<https://doi.org/10.1111/jfr3.12899>
- Hooke, J. (2016). Geomorphological impacts of an extreme flood in SE Spain. *Geomorphology*, 263, 19–38. <https://doi.org/10.1016/j.geomorph.2016.03.021>
- IndexPresse Business Etude. (2022). Économie maritime Les enjeux environnementaux et le numérique renouvellent une filière en pleine croissance. In *IndexPresse Business Etude* [Report].
- Jaiswal, R. K., Ali, S., & Bharti, B. (2020). Comparative evaluation of conceptual and physical rainfall–runoff models. *Applied Water Science*, 10(1).  
<https://doi.org/10.1007/s13201-019-1122-6>
- Jehanzaib, M., Ajmal, M., Achite, M., & Kim, T. (2022). Comprehensive Review: Advancements in Rainfall-Runoff Modelling for Flood Mitigation. *Climate*, 10(10), 147. <https://doi.org/10.3390/cli10100147>
- Jin, E., Wang, Y., Xu, Z., Yan, X., & Wang, X. (2023). Hydrometeorological-modeling-based analysis and risk assessment of a torrential rainfall flash flood in a data deficient area in Wenchuan County, Sichuan Province, China. *Stochastic Environmental Research and Risk Assessment*, 38(1), 33–50.  
<https://doi.org/10.1007/s00477-023-02553-7>
- Kantoush, S. A., Saber, M., Abdel-Fattah, M., & Sumi, T. (2021). Integrated Strategies for the management of Wadi flash floods in the Middle East and North Africa (MENA) arid Zones: the ISFF Project. In *Natural disaster science and mitigation engineering: DPRI reports* (pp. 3–34). [https://doi.org/10.1007/978-981-16-2904-4\\_1](https://doi.org/10.1007/978-981-16-2904-4_1)
- Karim, F., Armin, M. A., Ahmedt-Aristizabal, D., Tyhsen-Smith, L., & Petersson, L. (2023). A review of hydrodynamic and machine learning approaches for flood inundation modeling. *Water*, 15(3), 566. <https://doi.org/10.3390/w15030566>

- Khaing, Z. M., Zhang, K., Sawano, H., Shrestha, B. B., Sayama, T., & Nakamura, K. (2019a). Flood hazard mapping and assessment in data-scarce Nyaungdon area, Myanmar. *PLoS ONE*, *14*(11), e0224558. <https://doi.org/10.1371/journal.pone.0224558>
- Khaing, Z. M., Zhang, K., Sawano, H., Shrestha, B. B., Sayama, T., & Nakamura, K. (2019b). Flood hazard mapping and assessment in data-scarce Nyaungdon area, Myanmar. *PLoS ONE*, *14*(11), e0224558. <https://doi.org/10.1371/journal.pone.0224558>
- Kling, H., & Gupta, H. (2009). On the development of regionalization relationships for lumped watershed models: The impact of ignoring sub-basin scale variability. *Journal of Hydrology*, *373*(3–4), 337–351. <https://doi.org/10.1016/j.jhydrol.2009.04.031>
- Korichi, K., Hazzab, A., & Atallah, M. (2016a). Flash floods risk analysis in ephemeral streams: a case study on Wadi Mekerra (northwestern Algeria). *Arabian Journal of Geosciences*, *9*(11). <https://doi.org/10.1007/s12517-016-2624-2>
- Korichi, K., Hazzab, A., & Atallah, M. (2016b). Flash floods risk analysis in ephemeral streams: a case study on Wadi Mekerra (northwestern Algeria). *Arabian Journal of Geosciences*, *9*(11). <https://doi.org/10.1007/s12517-016-2624-2>
- Kouidri, K., Abdesselam, M., & Nekkache, G. A. (2019). Long-term seasonal characterization of extreme drought and flooding variability and their evolution in northwest Algeria. *Meteorology Hydrology and Water Management*, *7*(2), 63–71. <https://doi.org/10.26491/mhwm/106101>
- Kumar, V., Sharma, K., Caloiero, T., Mehta, D., & Singh, K. (2023). Comprehensive Overview of flood modeling Approaches: A review of recent advances. *Hydrology*, *10*(7), 141. <https://doi.org/10.3390/hydrology10070141>

- Leaffer, R. (2016). Mare clausum. In Serge Dauchy, Georges Martyn, Anthony Musson, Heikki Pihlajamäki, & Alain Wijffels (Eds.), *The Formation and Transmission of Western Legal Culture. 150 Books that Made the Law in the Age of Printing* (Vols. 7–7, pp. 190–194). Springer Verlag.
- Lee, J., Perera, D., Glickman, T., & Taing, L. (2020). Water-related disasters and their health impacts: A global review. *Progress in Disaster Science*, 8, 100123.  
<https://doi.org/10.1016/j.pdisas.2020.100123>
- Lee, S., Kang, T., Jin, Y., & Hwang, D. (2023). A case study on simulation of urban inundation by inland flooding and river flooding. *Korean Society of Hazard Mitigation*, 23(5), 31–42. <https://doi.org/10.9798/kosham.2023.23.5.31>
- Lehbab-Boukezzi, Z., Boukezzi, L., & Errih, M. (2016). Uncertainty analysis of HEC-HMS model using the GLUE method for flash flood forecasting of Mekerra watershed, Algeria. *Arabian Journal of Geosciences*, 9(20). <https://doi.org/10.1007/s12517-016-2771-5>
- Lindsay, J. B., & Seibert, J. (2012). Measuring the significance of a divide to local drainage patterns. *International Journal of Geographical Information Science*, 27(7), 1453–1468. <https://doi.org/10.1080/13658816.2012.705289>
- Liu, W., Feng, Q., Engel, B. A., Yu, T., Zhang, X., & Qian, Y. (2023). A probabilistic assessment of urban flood risk and impacts of future climate change. *Journal of Hydrology*, 618, 129267. <https://doi.org/10.1016/j.jhydrol.2023.129267>
- Liu, Z., Wang, Y., Xu, Z., & Duan, Q. (2019). Conceptual Hydrological Models. In *Springer eBooks* (pp. 389–411). [https://doi.org/10.1007/978-3-642-39925-1\\_22](https://doi.org/10.1007/978-3-642-39925-1_22)
- Loudyi, D., & Kantoush, S. A. (2020). Flood risk management in the Middle East and North Africa (MENA) region. *Urban Water Journal*, 17(5), 379–380.  
<https://doi.org/10.1080/1573062x.2020.1777754>

- Madi, H., & Bidjaoui, A. (2024). Engineering challenges in flash flood mitigation: insights from historical data and community perceptions in Tamanghasset, Algeria. *STUDIES IN ENGINEERING AND EXACT SCIENCES*, 5(2), e6906.  
<https://doi.org/10.54021/seesv5n2-111>
- Mardaid, E., Abidin, Z. Z., Asmai, S. A., & Abas, Z. A. (2023). Implementation of Flood Emergency Response System with Face Analytics. *International Journal of Advanced Computer Science and Applications*, 14(1).  
<https://doi.org/10.14569/ijacsa.2023.0140143>
- Maref, N., & Seddini, A. (2018a). Modeling of flood generation in semi-arid catchment using a spatially distributed model: case of study Wadi Mekerra catchment (Northwest Algeria). *Arabian Journal of Geosciences*, 11(6). <https://doi.org/10.1007/s12517-018-3461-2>
- Maref, N., & Seddini, A. (2018b). Modeling of flood generation in semi-arid catchment using a spatially distributed model: case of study Wadi Mekerra catchment (Northwest Algeria). *Arabian Journal of Geosciences*, 11(6). <https://doi.org/10.1007/s12517-018-3461-2>
- Merz, B., Blöschl, G., Vorogushyn, S., Dottori, F., Aerts, J. C. J. H., Bates, P., Bertola, M., Kemter, M., Kreibich, H., Lall, U., & Macdonald, E. (2021). Causes, impacts and patterns of disastrous river floods. *Nature Reviews Earth & Environment*, 2(9), 592–609. <https://doi.org/10.1038/s43017-021-00195-3>
- Mohanta, A., Patra, K. C., & Sahoo, B. B. (2018). Anticipate Manning's coefficient in meandering compound channels. *Hydrology*, 5(3), 47.  
<https://doi.org/10.3390/hydrology5030047>

- Mudashiru, R. B., Sabtu, N., Abustan, I., & Balogun, W. (2021). Flood hazard mapping methods: A review. *Journal of Hydrology*, *603*, 126846.  
<https://doi.org/10.1016/j.jhydrol.2021.126846>
- Munawar, H. S., Hammad, A. W. A., & Waller, S. T. (2022). Remote Sensing Methods for Flood Prediction: A review. *Sensors*, *22*(3), 960. <https://doi.org/10.3390/s22030960>
- Nastiti, K. D., An, H., Kim, Y., & Jung, K. (2018). Large-scale rainfall–runoff–inundation modeling for upper Citarum River watershed, Indonesia. *Environmental Earth Sciences*, *77*(18). <https://doi.org/10.1007/s12665-018-7803-x>
- Nastiti, K. D., Kim, Y., Jung, K., & An, H. (2015). The application of Rainfall-Runoff-Inundation (RRI) model for inundation case in Upper Citarum Watershed, West Java-Indonesia. *Procedia Engineering*, *125*, 166–172.  
<https://doi.org/10.1016/j.proeng.2015.11.024>
- Nations Unies. (1982). CONVENTION DES NATIONS UNIES SUR LE DROIT DE LA MER [Treaty]. In *Nations Unies, Recueil des Traités*.  
<https://treaties.un.org/doc/Publication/MTDSG/Volume%20II/Chapter%20XXI/XXI-6.fr.pdf>
- Nucera, A., Foti, G., Canale, C., Puntorieri, P., & Minniti, F. (2018). COASTAL FLOODING: DAMAGE CLASSIFICATION AND CASE STUDIES IN CALABRIA, ITALY. *WIT Transactions on Engineering Sciences*, *1*, 93–103.  
<https://doi.org/10.2495/risk180081>
- Obeidat, M., Awawdeh, M., & Al-Hantouli, F. (2021). Morphometric analysis and prioritisation of watersheds for flood risk management in Wadi Easal Basin (WEB), Jordan, using geospatial technologies. *Journal of Flood Risk Management*, *14*(2).  
<https://doi.org/10.1111/jfr3.12711>

- Olaleye, O., Akintola, O., Jimoh, R., Gbadebo, O., & Faloye, O. (2024). REVIEW AND COMPARATIVE STUDY OF HYDROLOGICAL MODELS FOR RAINFALL-RUNOFF MODELLING. *International Journal of Environment and Geoinformatics*, 11(3), 119–129. <https://doi.org/10.30897/ijegeo.1514176>
- Petrochenko, O. V. (2023). The problem of flooding and analysis of the ways of its solution. *Environmental Safety and Natural Resources*, 46(2), 5–22. <https://doi.org/10.32347/2411-4049.2023.2.5-22>
- Qu, Y., & Duffy, C. J. (2007). A semidiscrete finite volume formulation for multiprocess watershed simulation. *Water Resources Research*, 43(8). <https://doi.org/10.1029/2006wr005752>
- Rai, P. K., Mohan, K., Mishra, S., Ahmad, A., & Mishra, V. N. (2014). A GIS-based approach in drainage morphometric analysis of Kanhar River Basin, India. *Applied Water Science*, 7(1), 217–232. <https://doi.org/10.1007/s13201-014-0238-y>
- Rasmy, M., Sayama, T., & Koike, T. (2019). Development of water and energy Budget-based Rainfall-Runoff-Inundation model (WEB-RRI) and its verification in the Kalu and Mundeni River Basins, Sri Lanka. *Journal of Hydrology*, 579, 124163. <https://doi.org/10.1016/j.jhydrol.2019.124163>
- Remini, B. (2023, December 26). *FLASH FLOODS IN ALGERIA*. REMINI | LARHYSS Journal P-ISSN 1112-3680 / E-ISSN 2521-9782. <http://larhyss.net/ojs/index.php/larhyss/article/view/13785/925>
- Ruegg, J., Yip, M. K., & Brial, F. (2023). Les devoirs de protection et de préservation du milieu marin selon la Convention des Nations Unies sur le droit de la mer à l'aune de la sentence du Tribunal arbitral du 12 juillet 2016. *Études Caribéennes*, 55. <https://doi.org/10.4000/etudescaribeennes.27220>

- Saber, M., Kantoush, S. A., Abdel-Fattah, M., Sumi, T., Moya, J. A., & Abdrabo, K. (2021). Flash Flood Modeling and Mitigation in Arid and Semiarid Basins: Case Studies from Oman and Brazil. In *Natural disaster science and mitigation engineering: DPRI reports* (pp. 355–381). [https://doi.org/10.1007/978-981-16-2904-4\\_13](https://doi.org/10.1007/978-981-16-2904-4_13)
- Sahu, M. K., Shwetha, H. R., & Dwarakish, G. S. (2023). State-of-the-art hydrological models and application of the HEC-HMS model: a review. *Modeling Earth Systems and Environment*, 9(3), 3029–3051. <https://doi.org/10.1007/s40808-023-01704-7>
- San, Z. M. L. T., Zin, W. W., Kawasaki, A., Acierto, R. A., & Oo, T. Z. (2020). Developing flood inundation map using RRI and SOBEK models: a case study of the Bago River Basin, Myanmar. *Journal of Disaster Research*, 15(3), 277–287. <https://doi.org/10.20965/jdr.2020.p0277>
- Sardou, M., & Petrucci, O. (2023). Assessment of flood mortality indices in a Mediterranean framework: A comparative analysis between western Algeria and southern Italy. *International Journal of Disaster Risk Reduction*, 97, 104035. <https://doi.org/10.1016/j.ijdrr.2023.104035>
- Sayama, T., Matsumoto, K., Kuwano, Y., & Takara, K. (2019). Application of Backpack-Mounted Mobile Mapping System and Rainfall–Runoff–Inundation Model for flash flood analysis. *Water*, 11(5), 963. <https://doi.org/10.3390/w11050963>
- Sayama, T., Ozawa, G., Kawakami, T., Nabesaka, S., & Fukami, K. (2012). Rainfall–runoff–inundation analysis of the 2010 Pakistan flood in the Kabul River basin. *Hydrological Sciences Journal*, 57(2), 298–312. <https://doi.org/10.1080/02626667.2011.644245>
- Sayama, T., Tatebe, Y., Iwami, Y., & Tanaka, S. (2015). Hydrologic sensitivity of flood runoff and inundation: 2011 Thailand floods in the Chao Phraya River basin. *Natural Hazards and Earth System Sciences*, 15(7), 1617–1630. <https://doi.org/10.5194/nhess-15-1617-2015>

- Sim, S., & Kim, H. (2024). An Urban Flood Model Development Coupling the 1D and 2D Model with Fixed-Time Synchronization. *Water*, *16*(19), 2726.  
<https://doi.org/10.3390/w16192726>
- Sun, Y., Yang, Y., Zhang, B., Zhang, X., Xu, Y., Xiang, Y., & Chen, J. (2023). Applicability of the modified Green-AMPT model based on suction head calculation in Water-Repellent soil. *Water*, *15*(16), 2925. <https://doi.org/10.3390/w15162925>
- Sung, E., Tsai, M., & Kang, S. (2015). FloodViZ: a Visual-Based Decision support System for flood hazard Warning. *Proceedings of the . . . ISARC*.  
<https://doi.org/10.22260/isarc2015/0099>
- Swarztrauber, S. A. (1970). *The three-mile limit of territorial seas: a brief history* (By American University). <http://hdl.handle.net/10945/15200>
- Tan, M. L., Gassman, P. W., Yang, X., & Haywood, J. (2020). A review of SWAT applications, performance and future needs for simulation of hydro-climatic extremes. *Advances in Water Resources*, *143*, 103662.  
<https://doi.org/10.1016/j.advwatres.2020.103662>
- Troutman, B. M. (1985). Errors and parameter estimation in Precipitation-Runoff Modeling: 1. Theory. *Water Resources Research*, *21*(8), 1195–1213.  
<https://doi.org/10.1029/wr021i008p01195>
- United Nations. (n.d.). United Nations Convention on the Law of the Sea. In *United Nations Convention on the Law of the Sea* (p. 21).  
[https://www.un.org/depts/los/convention\\_agreements/texts/unclos/unclos\\_e.pdf](https://www.un.org/depts/los/convention_agreements/texts/unclos/unclos_e.pdf)
- United Nations. (1994). United Nations Convention on the Law of the Sea. In *United Nations - Treaty Series Nations Unies - Recueil Des Traités* (Vol. 1834, pp. 1–31363).  
[https://www.un.org/depts/los/convention\\_agreements/texts/unclos/unclos\\_f.pdf](https://www.un.org/depts/los/convention_agreements/texts/unclos/unclos_f.pdf)

- United Nations, Division for Ocean Affairs and the Law of the Sea, & Office of Legal Affairs. (2010). *The Law of the Sea*. United Nations.
- United States Office of Coast Survey. (2013). HISTORY OF THE MARITIME ZONES UNDER INTERNATIONAL LAW FROM THE CANNON SHOT RULE TO UNCLOS. In *Law of the Sea*.  
[https://www.nauticalcharts.noaa.gov/staff/law\\_of\\_sea.html](https://www.nauticalcharts.noaa.gov/staff/law_of_sea.html)
- Waikar, M. L., & Nilawar, A. P. (2014). Morphometric Analysis of a Drainage Basin Using Geographical Information System: A Case study [Journal-article]. *Int. J. of Multidisciplinary And Current Research*, 2, 179–180. <http://ijmcr.com/wp-content/uploads/2014/02/Paper32179-184.pdf>
- Wang, J., Hong, Y., Li, L., Gourley, J. J., Khan, S. I., Yilmaz, K. K., Adler, R. F., Policelli, F. S., Habib, S., Irwn, D., Limaye, A. S., Korme, T., & Okello, L. (2011). The coupled routing and excess storage (CREST) distributed hydrological model. *Hydrological Sciences Journal*, 56(1), 84–98. <https://doi.org/10.1080/02626667.2010.543087>
- Wang, X., Goreville, P., & Liu, C. (2023). Flash Floods: Forecasting, monitoring and Mitigation Strategies. *Water*, 15(9), 1700. <https://doi.org/10.3390/w15091700>
- Wardhani, F. A., Sapan, E. G. A., Widiatmoko, N., Yuvhendmindio, M. R., Santosa, B. H., Susanti, W. D., Pravitasari, A. E., Triwisesa, E., & Ridwansyah, I. (2024). Comparative assessment of a flash flood susceptibility map based on morphometric analysis and bivariate statistics in the Upper Citarum Watershed, Indonesia. *Bulletin of Geography Physical Geography Series*, 27, 87–109. <https://doi.org/10.12775/bgeo-2024-0012>
- Wasimi, S. A. (2010). Climate change in the Middle East and North Africa (MENA) region and implications for water resources project planning and management. *International*

*Journal of Climate Change Strategies and Management*, 2(3), 297–320.

<https://doi.org/10.1108/17568691011063060>

Weber, A.-P. & Académie des sciences d'outre-mer. (2014). Régence d'Alger et royaume de France, 1500-1800 : trois siècles de luttes et d'intérêts partagés. In *Les Recensions De L'Académie*. éd. l'Harmattan.

Yao, S., Chen, N., Du, W., Wang, C., & Chen, C. (2021). A cellular automata based Rainfall-Runoff model for urban inundation analysis under different land uses. *Water Resources Management*, 35(6), 1991–2006. <https://doi.org/10.1007/s11269-021-02826-2>

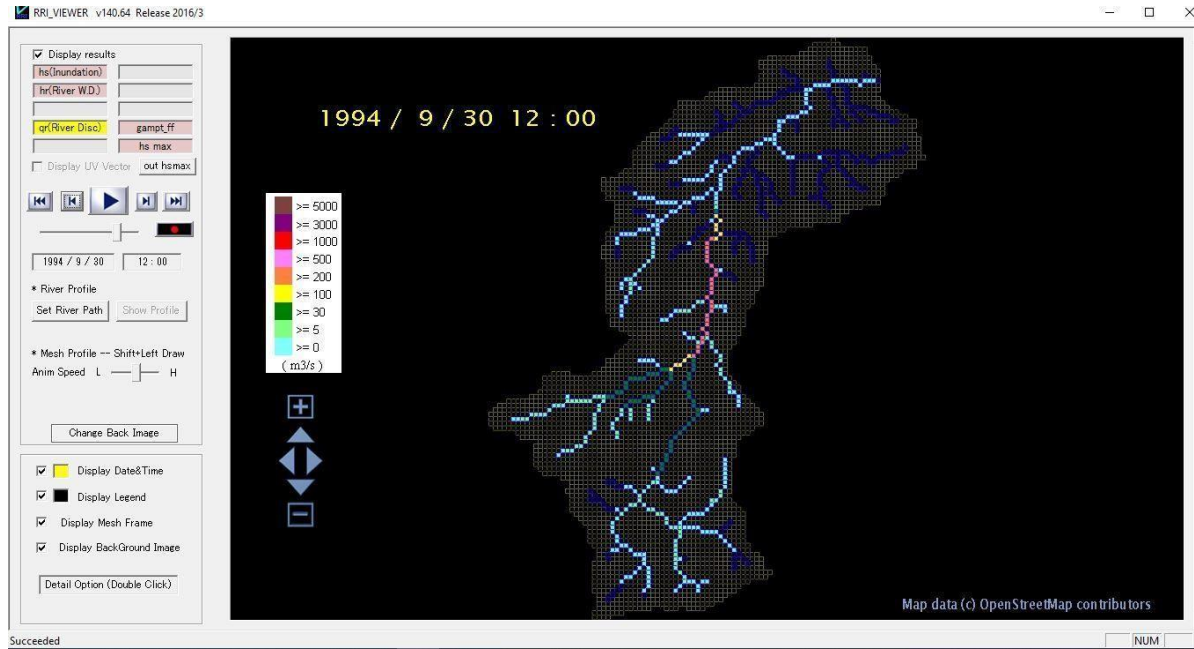
Zouai, F., Bouhelal, S., Cagiao, M. E., Benabid, F. Z., Benachour, D., & Calleja, F. J. B. (2014). Study of nanoclay blends based on poly(ethylene terephthalate)/poly(ethylene naphthalene 2,6-dicarboxylate) prepared by reactive extrusion. *Journal of Polymer Engineering*, 34(5), 431–439. <https://doi.org/10.1515/polyeng-2013-0244>

## APPENDIX

Table 2.3: Detailed description of conceptual, physical and empirical models (Jehanzaib et al., 2022).

Categories	Characteristics	Strengths	Weaknesses	Models
<b>Conceptual model</b>	<ul style="list-style-type: none"> <li>- Parametric or grey-box model.</li> <li>- Incorporate semi-empirical equations grounded in physical principles.</li> <li>- Parameters are obtained from calibration and field data.</li> <li>- Straightforward and readily executable on computers.</li> <li>- Necessitate extensive hydro-meteorological data.</li> <li>- Calibration entails curve fitting, complicating physical interpretation.</li> </ul>	<ul style="list-style-type: none"> <li>- Effortless calibration, uncomplicated model architecture.</li> <li>- Adjust using restricted data.</li> <li>- Require reduced computational effort.</li> </ul>	<ul style="list-style-type: none"> <li>- Fails to account for spatial variations within the catchment area.</li> <li>- Not advisable for extensive catchments.</li> </ul>	SM,TANK, GR2M,GR4 J,ABCD,H BV
<b>Physical model</b>	<ul style="list-style-type: none"> <li>-Mechanistic or white-box model.</li> <li>-Grounded on spatial distribution, assessment of parameters delineating physical qualities.</li> <li>-The model is intricate and necessitates human expertise and computational capacity.</li> <li>-Necessitates information regarding the initial condition of the model and the morphology of the catchment area.</li> <li>-Illustrates various hydrological processes via equations of mass, momentum, and energy conservation</li> </ul>	<ul style="list-style-type: none"> <li>- Integrates geographical and temporal variability at a very fine scale.</li> <li>- Applicable to a broad spectrum of scenarios.</li> </ul>	<ul style="list-style-type: none"> <li>- Experience issues linked to scaling.</li> <li>- A substantial quantity of parameters and calibration is required; site-specific.</li> </ul>	WATFLOOD,SWMM, HEC-HMS,TOP MODEL
<b>Empirical model</b>	<ul style="list-style-type: none"> <li>-Data-driven or metric-based model.</li> <li>-Utilise mathematical formulae, extract value from existing time series data.</li> <li>-Minimal attention to the characteristics and mechanisms of the system.</li> <li>-Cannot be produced for other catchments.</li> <li>-Applicable within the confines of the specified domain</li> </ul>	<ul style="list-style-type: none"> <li>- Minimal parameters required.</li> <li>- Minimal data necessity.</li> <li>- Applicable in ungauged catchments.</li> </ul>	<ul style="list-style-type: none"> <li>- Absence of correlation among physical catchment, input data distortion, or Black-box.</li> <li>- Elevated computational expense and duration.</li> </ul>	SCS-CN, ANN, UH

A1: simulation of runoff (Mekerra watershed) using RRI model.



## A2: Water depth and river discharge using RRI model.

